

General Disclaimer

One or more of the Following Statements may affect this Document

- This document has been reproduced from the best copy furnished by the organizational source. It is being released in the interest of making available as much information as possible.
- This document may contain data, which exceeds the sheet parameters. It was furnished in this condition by the organizational source and is the best copy available.
- This document may contain tone-on-tone or color graphs, charts and/or pictures, which have been reproduced in black and white.
- This document is paginated as submitted by the original source.
- Portions of this document are not fully legible due to the historical nature of some of the material. However, it is the best reproduction available from the original submission.

NASA Contractor Report 172570

Box Truss Analysis and Technology Development Task 1 Mesh Analysis and Control

E. E. Bachtell, S. S. Bettadapur, J. V. Coyner

Martin Maritta Aerospace
Denver Aerospace
P.O. Box 179
Denver, CO 80201

Contract NAS1-17551
August 1985

(NASA-CR-172570) BOX TRUSS ANALYSIS AND
TECHNOLOGY DEVELOPMENT. TASK 1: MESH
ANALYSIS AND CONTROL Final Report (Martin
Marietta Aerospace) 118 p HC A b/MF A/1

N85-34156

CSCL 22B 13/18

Unclas

22265



NASA

National Aeronautics and
Space Administration

Langley Research Center
Hampton, Virginia 23665

NASA Contractor Report 172570

**Box Truss Analysis and Technology
Development
Task 1
Mesh Analysis and Control**

E. E. Bachtell, S. S. Bettadapur, J. V. Coyner

**Martin Maritta Aerospace
Denver Aerospace
P.O. Box 179
Denver, CO 80201**

**Contract NAS1-17551
August 1985**

NASA

National Aeronautics and
Space Administration

Langley Research Center
Hampton, Virginia 23665

FOREWORD

This report was prepared by Martin Marietta Denver Aerospace under Contract NAS1-17551. This report covers the results of Task 1. The contract was administered by the Langley Research Center of the National Aeronautics and Space Administration. The Task 1 study was performed from February 1984 to January 1985 and the NASA-LaRC project manager was Mr. U. M. Lovelace.

CONTENTS

	<u>Page</u>
1.0 INTRODUCTION	1
1.1 Box Truss Antenna System	1
1.2 Direct Tieback System	3 thru 5
2.0 USING THE MESH INTEGRATED ANALYSIS SYSTEM	6
2.1 Analysis Techniques	10
2.1.1 Worst-Case Analysis	10
2.1.2 One-Dimensional Interpolation	10
2.1.3 Two-Dimensional Interpolation	12
2.1.4 Interpolation Limitations	14
2.2 Tie Spacing	16
2.3 Manufacturing Tolerance	17
2.4 Limitations	17
3.0 MESH TIE SYSTEM GENERATOR	18
3.1 Top of Standoffs and Standoff Heights	18
3.2 Tie Spacing	22
3.3 Tie System	24
3.3.1 Creation of Cross Points and Cross Cords	24
3.3.2 Creation of Radial Tie Points and Surface Cords	26
3.3.3 Creation of Tieback Cords	28
3.4 Element Sectional and Material Properties	28
3.5 Tie System Analytical Model	29
3.5.1 Reduced Analytical Model Accuracy	31
3.6 Determination of Initial Strain	32 thru 34
4.0 LOAD GENERATOR	35
4.1 Nodal Loads	35
4.2 Nodal Constraints	36
4.3 Pressure and G-Loads	36
4.4 Temperatures	37
5.0 MODEL OPTIMIZER	38 thru 40
6.0 FINITE-ELEMENT MODEL SOLVER	41
6.1 Pretension Condition	41
6.2 Nonlinear Effects	42
6.3 Pressure Loading	45
6.3.1 Z Component of Pressure	45
6.3.2 Y Component of Pressure	46
6.3.3 X Component of Pressure	48 thru 50
7.0 SURFACE TOPOGRAPHY SOLVER	51
7.1 Interpolation Routine	51
7.2 "Best-Fit" Surface Routine	52 thru 54

8.0	RF PERFORMANCE SOLVER	55
8.1	Aperture Integration	55
8.2	Rotating Grid Method	56
8.3	Geometry for the Reflector Surfaces	56
8.4	Calculation of the Aperture Fields	57
8.4.1	Ray Tracing	59
8.5	Beam Efficiency	62
		and 63
9.0	MESH CONTROL	64
9.1	Analysis Method	66
9.2	EOS Tie System Design	67
9.3	Analysis Cases	69
9.4	Analysis Results	70
		thru 72
10.0	SUMMARY	73
		and 74
	APPENDIX A	A-1
		thru A-32
	APPENDIX B	B-1
		thru B-4

Figure

1	Deployable Box Truss Schematic	2
2	Box Truss Antenna System	3
3	Box Truss and Direct Tieback Tie System	4
4	Integrated Mesh Analysis System	6
5	Typical One-Dimensional Loading	11
6	Typical Two-Dimensional Loading	13
7	Typical Interpolation Limited Loading	15
8	Coordinate System--Offset Fed Antenna	19
9	Coordinate System--Center Fed Antenna	19
10	Cutaway--Offset Fed Antenna Location of Tops of Standoffs	20
11	Box Section and Tops of Standoffs Number Scheme	21
12	Standoff Height Determination	22
13	Cutaway Section of a Typical Paraboloidal Reflector	23
14	Renumbering of Standoffs	25
15	Creation of Cross Points	25
16	Creation of Cross Cords	26
17	Tie Point Numbering Scheme	27
18	Surface Cord Numbering Scheme	27
19	Standoff Cross Section	29
20	Initially Strained Cords	32
21	Typical Unoptimized Interconnectivity Matrix	39
22	Typical Optimized Interconnectivity Matrix	40
23	Typical Cable Element	44
24	Newton-Raphson Solution	44
25	X-Y Plane Projection	46
26	X-Z Plane Projection	47

27	Y-Z Plane Projection	49
28	Surface Movements	53
29	Coordinate System for a Surface Revolution	57
30	Geometry of Ray Tracing to Aperture Field Point	58
31	Reflection Point XP, and Its Estimate XPO	60
32	Local Coordinates at XPO on a Doubly Curved Surface	61
33	EOS Spacecraft	65
34	Typical Linear Actuator System	66
35	60-Meter Section of EOS	68
36	Standoff Member	69

Table

1	Summary of the Mesh Tie System Generator	8
2	Summary of the Loadcase Generator	9
3	Summary of the Model Optimizer, Model Solver, Surface Topography Solver, and rf Performance Solver	9
4	Material Properties for Graphite and Quartz Cords	28
5	Design Parameters and Model Size	31
6	Finite Element Results	31
7	Tie System Model Generator Inputs	69
8	Temperature Values on Mesh Tie Cords	70
9	Temperature Values on Standoffs	70
10	Standoff Movement to Adjust for Surface Distortions	70
11	Results of Onorbit Surface Adjustment	72

A very accurate reflective surface is vital to the performance of large box truss reflector antennas. For large antenna systems to work, the surface accuracy, D/σ , is required to be greater than 5×10^4 , where D = antenna diameter and σ = surface rms error. One of the most time consuming and costly phases in designing and analyzing a box truss antenna is the design and analysis of the mesh reflective surface and mesh tie system. Previously, the design and analysis of a particular tie system configuration required excessive man-hours and computer time. Much of the design and analysis process was hand generated, therefore, changing a design quickly was difficult.

The solution to this problem has been the development of a Integrated Mesh Analysis System to model, analyze, and predict rf performance for box truss antennas with reflective mesh surfaces. This analysis system was commissioned by NASA under the Box Truss Analysis and Technology Development task contract, Task 1 Mesh Analysis and Control. It is unique in that it integrates custom written programs for cord-tied mesh surfaces, thereby drastically reducing both the man-hours and computer dollars required to design and analyze mesh antennas. In addition to the Mesh Integrated Analysis System for box truss mesh reflector antennas, a parametrics study using the mesh analysis system was performed to determine the effects of onorbit calibration, i.e., surface adjustment on a typical box truss antenna. The baseline antenna used in the study was the Earth Observation Spacecraft (EOS), NASA CR-3698. Chapter 9.0 describes the parametric study on onorbit calibration.

1.1 BOX TRUSS ANTENNA SYSTEM

The basic box truss structure was first designed and used on the On-orbit Assembly (OOA) program, Contract No. F04701077-C-018C, for the Air Force (Fig. 1). OOA used the box truss structure to design a planar truss system to support a mesh array. Mesh support posts or standoffs were used to separate the radiating surface from the support structure. The separation provides the volume necessary to stow the mesh and mesh tie-system and to assure that neither the mesh or tie cords will impinge on the deployment of the box truss. Generally, the standoffs are tubes of similar cross section to the box truss vertical members and are inserted into the corner fittings. The mesh is attached to the top of the standoffs. In 1979, an IR&D study was performed to determine the adaptability of the box truss to nonplanar shapes, i.e., parabolic and spherical reflector systems. The conclusions of that study were as follows:

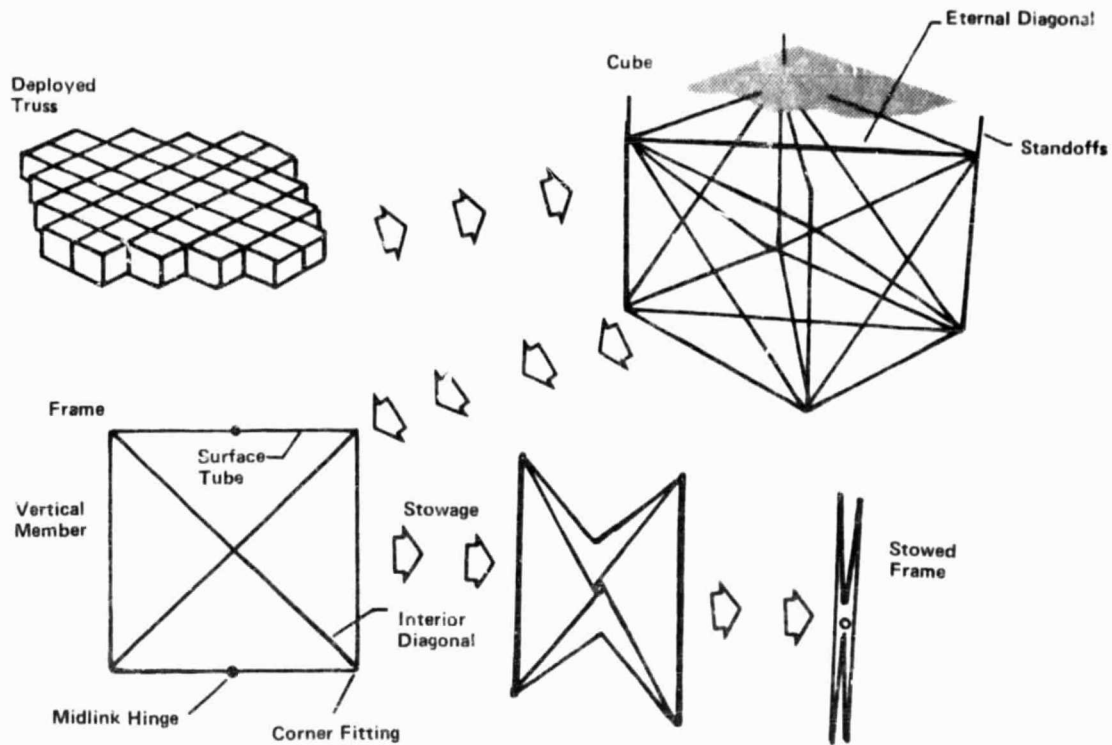


Figure 1 Deployable Box Truss Schematic

- 1) The vertical members on the box truss structure must be vertical rather than perpendicular to the surface to assure step-by-step deployment and stowability;
- 2) The paraboloid of revolution was the only nonflat surface that can be formed by a box truss structure using equal length standoffs.

To achieve the parabolic curve shape, each box truss face consisting of two vertical members and two surface tubes are sheared by using different length interior diagonal members. However, because of the close approximation between a paraboloid and sphere, a spherical reflector can be formed by using a parabolic box truss reflector support structure and varying the mesh standoff heights. Figure 2 shows a section cut of a box truss structure used to support either a parabolic or spherical mesh reflector surface. This figure illustrates that for the parabolic reflector each standoff is a fixed length, while the standoffs for the spherical surface vary by the difference between a sphere and paraboloid. The Integrated Mesh Analysis System uses this design approach to determine the coordinates for the top and bottom of each standoff in the reflector.

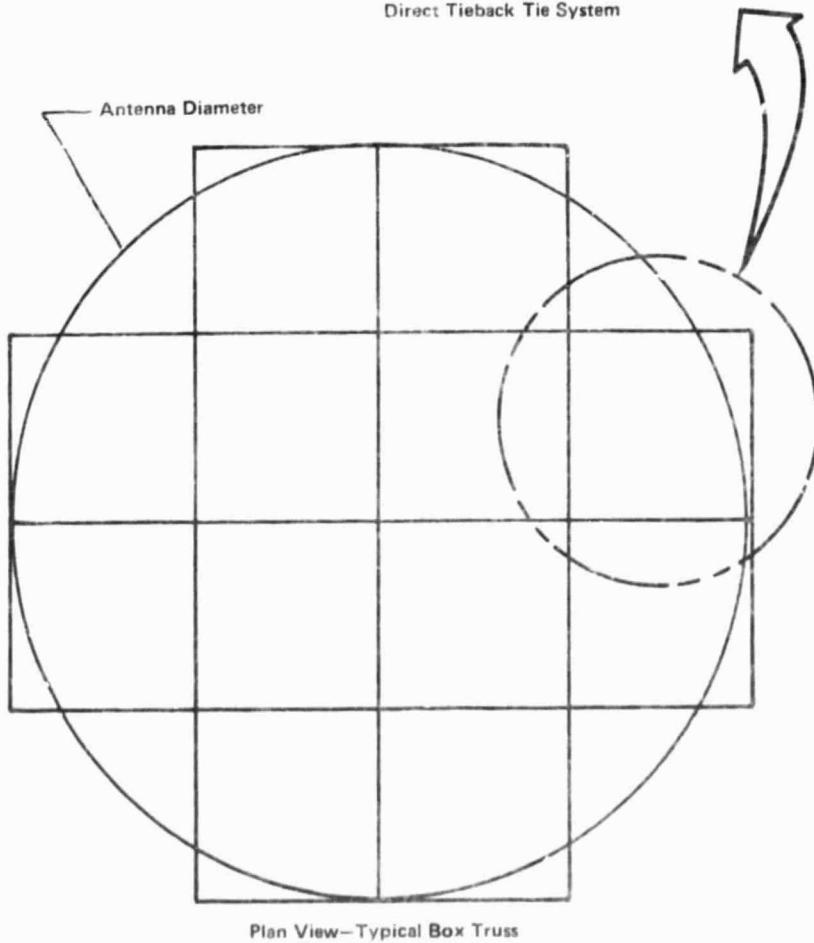
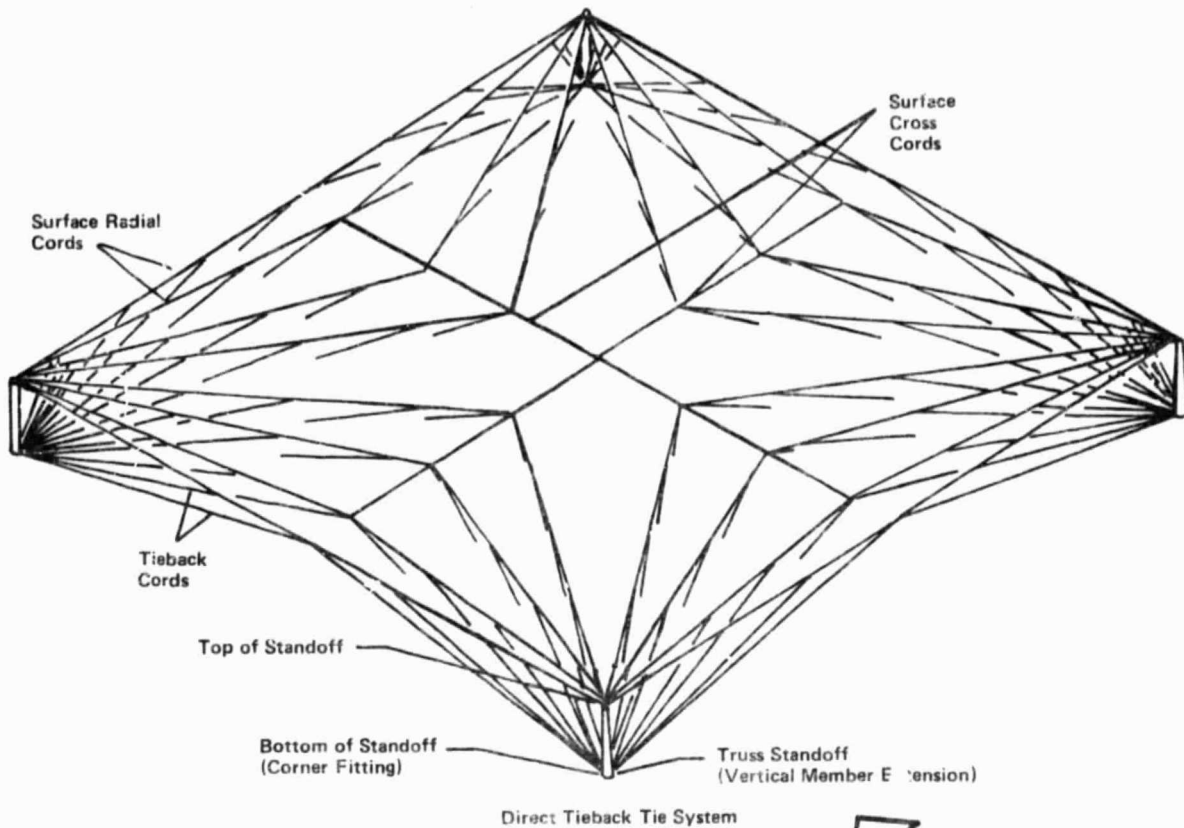


Figure 3 Box Truss and Direct Tieback Tie System

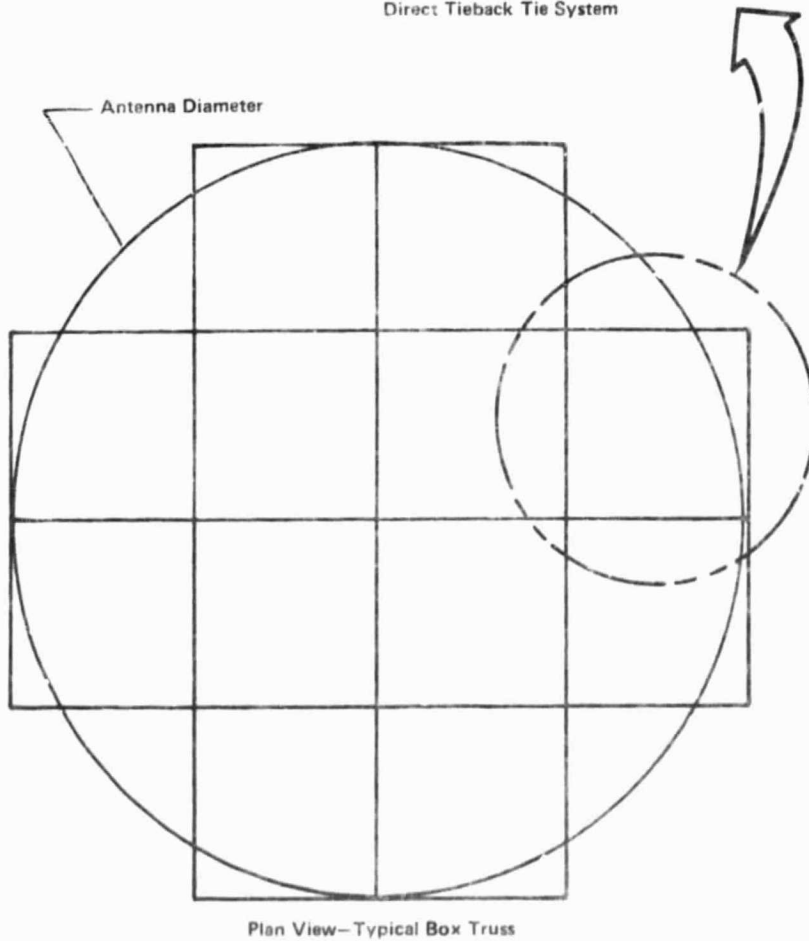
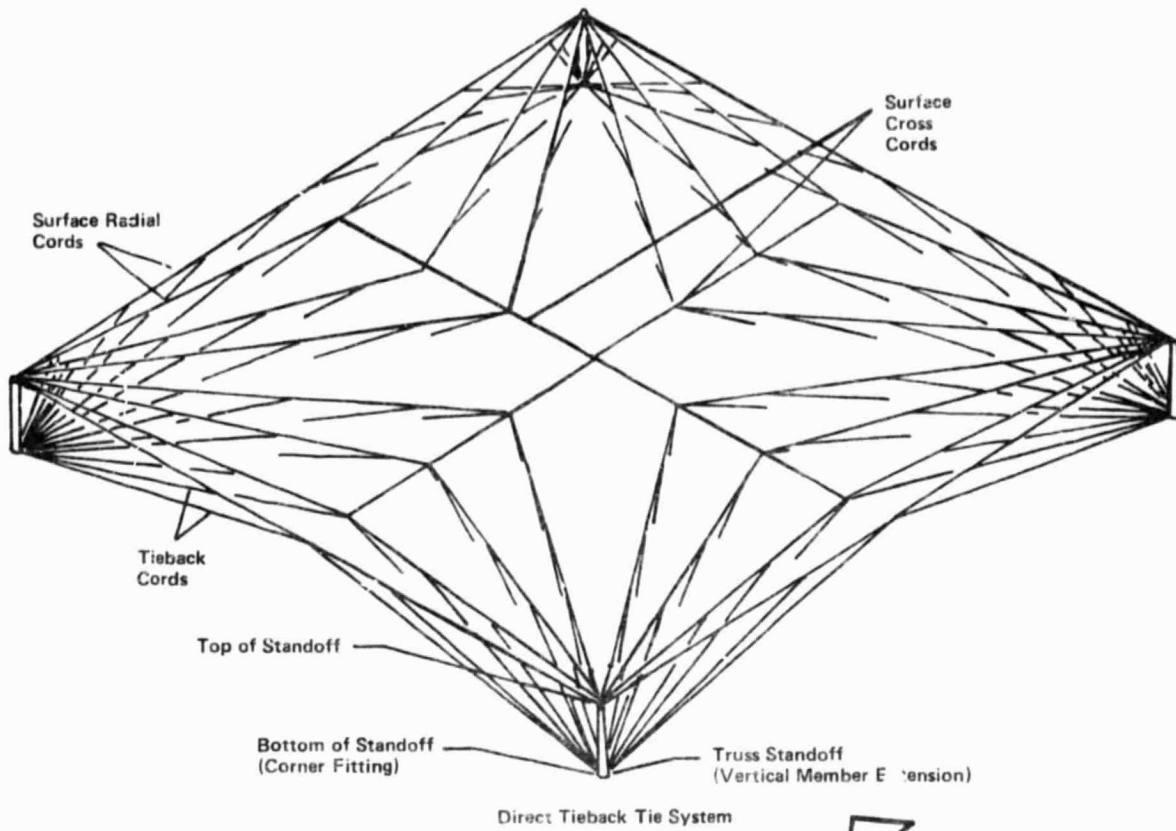


Figure 3 Box Truss and Direct Tieback Tie System

Figure 3 shows that the direct tieback system consists of three types of cords: the surface cross cords that bisect the mesh reflective surface; the surface radial cords that extend radially from the top of the standoffs to the surface cross cords; and the tieback cords that extend from the surface cords to the bottom of the standoffs. The bottom of the standoffs correspond to the location of the corner fittings on the box truss. The tieback cords are used to pull the surface into shape and are tied along each surface cord at a distance defined as the tie spacing. Note that the cross cords do not span the entire width of the box section. This is necessary to enable the tie system of each box section to be manufactured separately. Also, this helps to eliminate most of the interaction between the tie systems of adjacent box sections, allowing each tie system of each box to operate independently. Consequently, this produces a more stable reflector surface since local environmental effects such as shadowing of a single box section will not effect the surface of other box sections. Since each tie system can operate independently, analyzing the complete reflective surface can be performed on a per box section basis. Section 2.1 describes this process.

The complete analysis system consists of six integrated computer programs (Fig. 4). The first two programs are interactive programs that provide the necessary inputs for the remaining batch process programs. Using the Integrated Mesh Analysis System to design and analyze a box truss mesh reflector consists of the following:

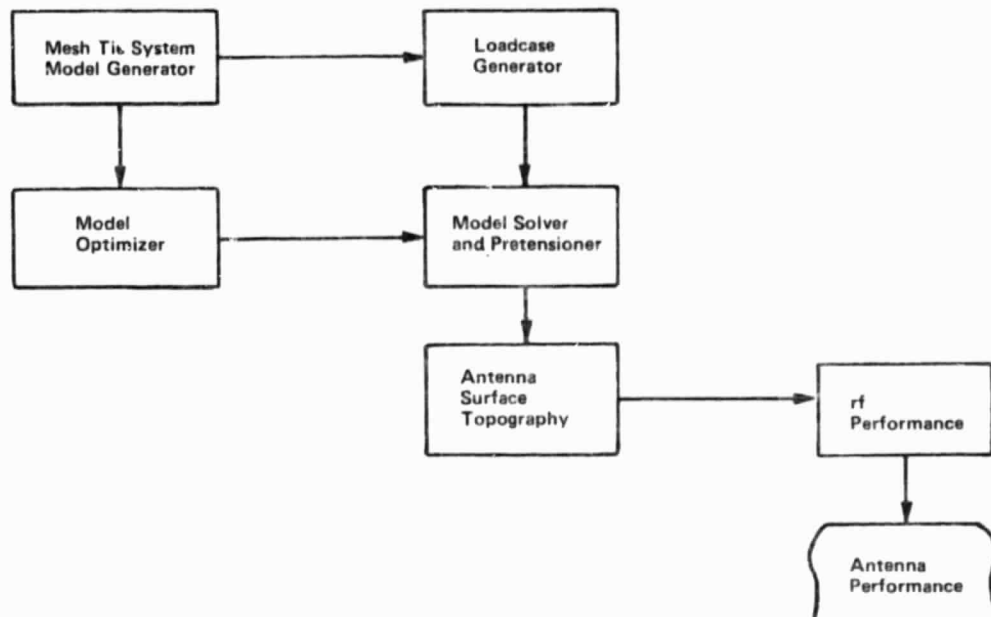


Figure 4 Integrated Mesh Analysis System

- 1) Using the mesh tie system generator, create the tie system design and finite-element model of the tie system.
- 2) Using the loadcase generator, create the loadcases to be placed on the tie system finite-element model. These loadcases can represent any operational or manufacturing environments, including the corresponding box truss displacements.
- 3) Using the model optimizer, generate the optimized finite-element input file for the model solver.
- 4) Using the model solver, determine the tie system distortions by solving the tie system finite-element model for the above specified loadcases.
- 5) Using the antenna surface topography solver, determine the best-fit parabolic surface, effective feed scan, axial defocus, and minimum rms surface error to match the surface distortions.

- 6) Using the rf performance solver, determine the far-field pattern, antenna gain, and beam efficiency of the antenna.

A precursor to running any of the above programs is to determine the necessary design and analysis parameters required by the various programs. First, the basic design parameters must be chosen, e.g., reflector diameter and focal length. Next, the analysis technique and box sections that will best determine the reflector's behavior to a particular environment must be chosen. The details of the available analysis techniques and when each technique should be used is discussed in Section 2.1. Finally, the operational and manufacturing conditions to be analyzed must be chosen. Each condition will be input as a separate loadcase in the loadcase generator. The loadcases should include the corresponding box truss support structure displacements that have been determined before running the Integrated Mesh Analysis System. As an example, to analyze a particular thermal environment, the box truss distortions would be determined before running these programs using a NASTRAN finite-element model of the box truss. The corner fitting distortions that result can then be applied to the mesh surface via specified displacements at the bottom of the standoffs. Section 4.2 discusses the details for inputting the specified displacements.

Appendix B provides an input data form to be filled out before running the mesh tie system generator. By filling out a copy of the form, the user will have all necessary inputs determined before running the program. After the tie system design and finite-element model have been generated, the user should create a form that can be used when running the loadcase generator to assist in defining each loadcase to be analyzed. Tables 1, 2, and 3 summarize each program that makes up the Integrated Mesh Analysis System. Tables 1 and 2 show the required and optional program inputs for the two interactive programs--the mesh tie system generator and the loadcase generator, respectively. Also, summarized are the program outputs and limitations. Table 3 summarizes the program function, operation, and outputs for the remaining batch process programs. The following sections discuss the guidelines for using the Mesh Integrated Analysis System effectively. Sections 3 through 8 describe each of the programs in detail. A user's manual for running all of the programs can be found in Appendix A.

Table 1 Summary of the Mesb Tie System Generator

Major Design Choices Specified by User (O) Optional (R) Required	Other Program Inputs (O) Optional (R) Required	Program Function, Operation, and Outputs	Program Limitations
1) Reflector Diameter (R) 2) Reflector Focal Length (R) 3) Reflector Type (R) A) Parabolic or Spherical B) Offset Fed or Center Fed 4) Box Truss Geometry (R) A) Square or Rectangular Box Sections B) Number of Box Sections C) Manufacturing Tolerance (R) D) Feed Type (R) E) db Edge Taper for Feed (R) F) Operating Frequency (R) G) Standoff Height (O) H) Tie Spacing (R) I) Surface Cord Material and Size (R) J) Tieback Cord Material and Size (R) K) Standoff Material and Cross Sectional Size (R)	1) Analysis Technique (R) A) Worst-Case B) One-Dimensional Interpolation C) Two-Dimensional Interpolation 2) Box Sections to Be Analyzed (R) 3) Reduction in Tie System Design to Be Analyzed (R) 4) Plotting Box Truss Geometry (O) 5) Plotting Tie System Geometry (O)	Interactive program used to design mesh-tie system and to define all necessary inputs for later programs. Outputs consist of interactive screen printouts that define the tie system configuration and coordinates. Also, program outputs files used to plot the box truss and ties system configuration and files used by other programs.	1) Antenna must have an $F/D > 0.3$. 2) Antenna must be made up of less than 25x25 box truss sections. 3) If analysis technique other than worst-case analysis is to be used all boxes must have a similar geometric shape, i.e., all square or all rectangular. 4) Analytical model of the tie system is limited to 145 tie points and 500 tie cord segments.

Table 2 Summary of the Loadcase Generator

Choices Specified by User	Program Function, Operation and Outputs
1) Number of Loadcases 2) Loadcase Type A) Type 0—Redefine all loadcase conditions. B) Type 1—Add element temperatures to previous point loads, constraints, pressures, and g-load conditions. May also be used to redefine previous temperature condition. 3) Nodal Point Loads 4) Nodal Constraints 5) Pressure Loads 6) g-loads 7) Element Temperatures	<p>A menu-driven interactive program used to define manufacturing or operational environments that will be analyzed for their effect on antenna performance.</p> <p>Outputs consist of interactive screen printouts and a single output file used by the Model Solver that defines the user's loadcases.</p>

Program has no limitations.

Table 3 Summary of the Model Optimizer, Model Solver, Surface Topography Solver, and rf Performance Solver

Program	Program Function, Operation, and Outputs
Model Optimizer	A batch process program used to optimize the nodal bandwidth of the finite-element model. Also, used to create the input deck for the Model Solver and a output file to be reviewed by the user to assure the tie system design has been defined correctly before running the Model Solver.
Model Solver	A batch process finite-element program used to solve distortions of the analyzed box sections for the loadcases defined in the loadcase generator. Output consists of two files. The first is the solution output for the user defining tie-point displacements, element forces, and reactions. The second is a file containing tie-point displacements only which is used by the Surface Topography Solver.
Surface Topography Solver	A batch process program used to interpolate tie-point distortions of the analyzed box truss sections onto the entire reflector surface. Also, this program determines the "best-fit" reflector for the distorted surface. Output consists of a single file that defines the resulting "best-fit" surface for each loadcase analyzed, including equivalent feed movement and rms surface errors. Also contained in this output file is a card image deck to be used as input into the rf Performance Solver.
Performance Solver	A batch process program that uses aperture integration to determine the far-field pattern and beam efficiency of the distorted reflector.

2.1 ANALYSIS TECHNIQUES

Ideally, analysis of a mesh tie system would involve the creation and analysis of the entire surface, i.e., the direct tie back system for the entire reflector area. However, to maximize cost effectiveness, the Integrated Mesh Analysis System creates and analyzes tie systems for individually specified box sections in conjunction with the type of analysis used. The following are the three types of analysis techniques available.

2.1.1 Worst-Case Analysis

This method allows for the creation and analysis of a single box section. It is the simplest and cheapest of the three methods. It is also the most conservative and is used primarily to determine the worst possible antenna performance. If this option is chosen, the mesh tie system generator will require the user to input a single box section to be analyzed. The optimum box sections for use in this analysis are those on the perimeter of the aperture. These box sections have the highest slopes, and the magnitude of their distortions resulting from any load environment is greater than for that of interior boxes. The worst possible loading environment should be used on this box section. The assumption is that all of the remaining box sections have similar distortions.

2.1.2 One-Dimensional Interpolation

One-dimensional interpolation is used in cases where loading conditions vary predominantly along one major antenna axis. The assumption here is that tie point distortions differ linearly in one direction and are constant in the other. The user is asked to choose two box sections for finite element analysis and a direction for interpolation. The tie point displacements obtained for these two box sections are linearly interpolated in the direction specified by the user to find the displacements of those boxes in between. Next, the line of displacements is spread as a constant in the transverse direction. Any boxes that deviate from this pattern can be incorporated in the form of shadowed boxes. A shadowed box is any box that has a unique loading environment, making individual finite element analysis necessary. These displacements replace their corresponding interpolated displacements on the surface. This ultimately gives displacements for the entire reflector surface.

As an example, one-dimensional interpolation can be used on the spacecraft in Figure 5. The thermal environments for all boxes along Line 1 are relatively the same. Therefore, it can be assumed that the tie system distortions for all boxes along Line 1 are equal. Similarly, the thermal environments for all boxes along any line are relatively equal, and it can be assumed that the distortions along that line are also equal. However, the thermal environments between lines are different. Therefore, one-dimensional interpolation can be used by analyzing any box in Line 1 and any box in Line 4, i.e., shaded box sections 101 and 403, and interpolating their displacements linearly for boxes in Lines 2 and 3. To analyze such a case, the user would input box numbers 101 and 403 and choose the X direction for interpolation.

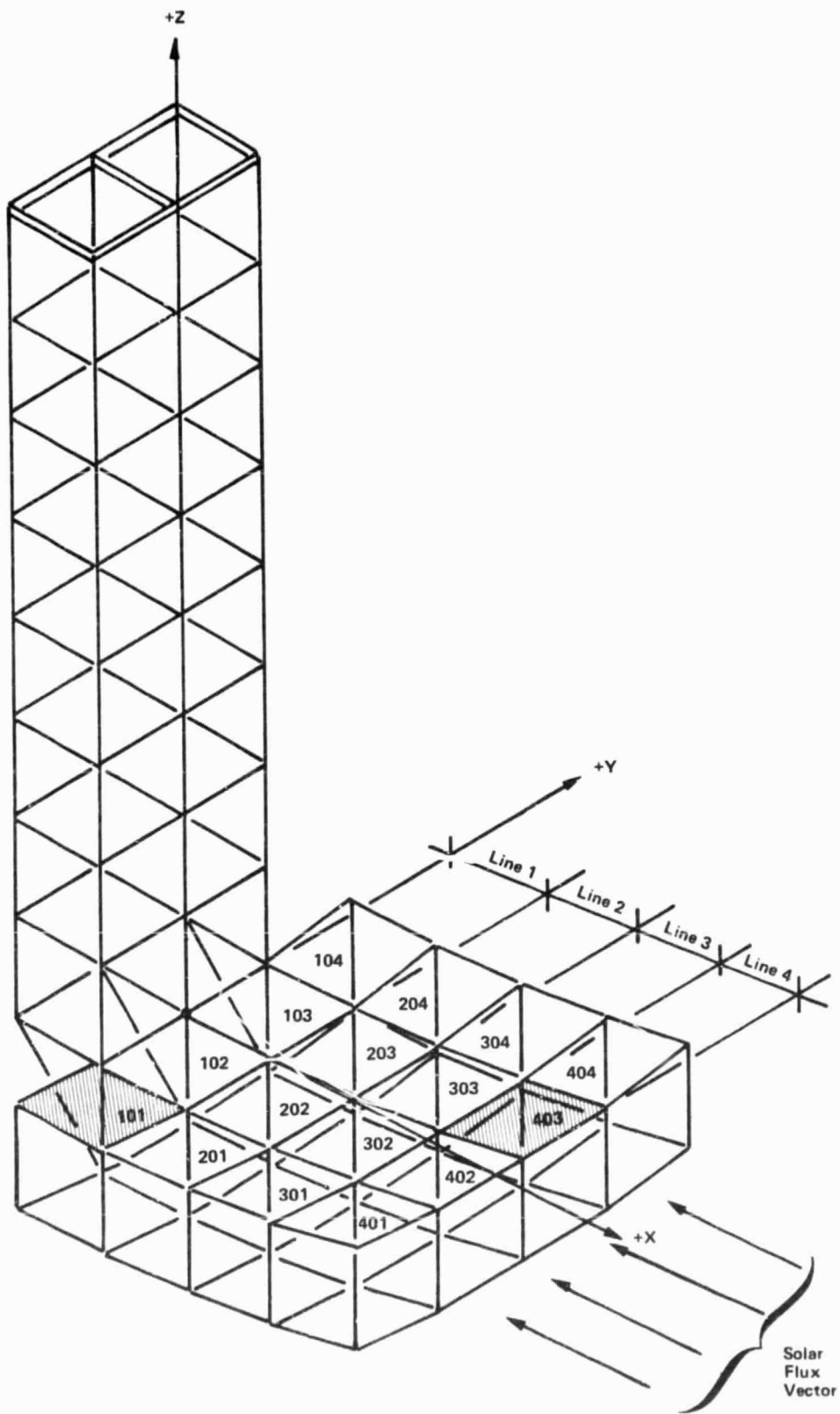


Figure 5 Typical One-Dimensional Loading

2.1.3 Two-dimensional Interpolation

Two-dimensional interpolation is used in cases where loading conditions vary along any direction. The assumption here is that tie point distortions differ linearly along the antenna's X and Y axes. The user is asked to choose four box sections for finite element analysis. Two of the box sections must be in line with one another in either the X or Y axis. The tie point displacements obtained for these two box sections are linearly interpolated to find the tie point displacements for those in between. This forms a line of displacements. Next, linear interpolation is performed between each of the remaining two box sections and the line of distortions, forming two transverse lines of distortions. Finally, interpolation is performed between these two lines resulting in tie point displacements for the entire surface. Shaded boxes are then included in the same manner as in one-dimensional interpolation.

As an example, two-dimensional interpolation can be used on the reflector in Figure 6. The thermal environment is such that distortions will vary along both the X and Y axes of the reflector. By choosing the shaded box sections for analysis, the distorted shape of the reflector can be determined using linear interpolation. Note that the requirement that two boxes must be in line with one another is met by defining boxes 101 and 401 as two of the four box sections.

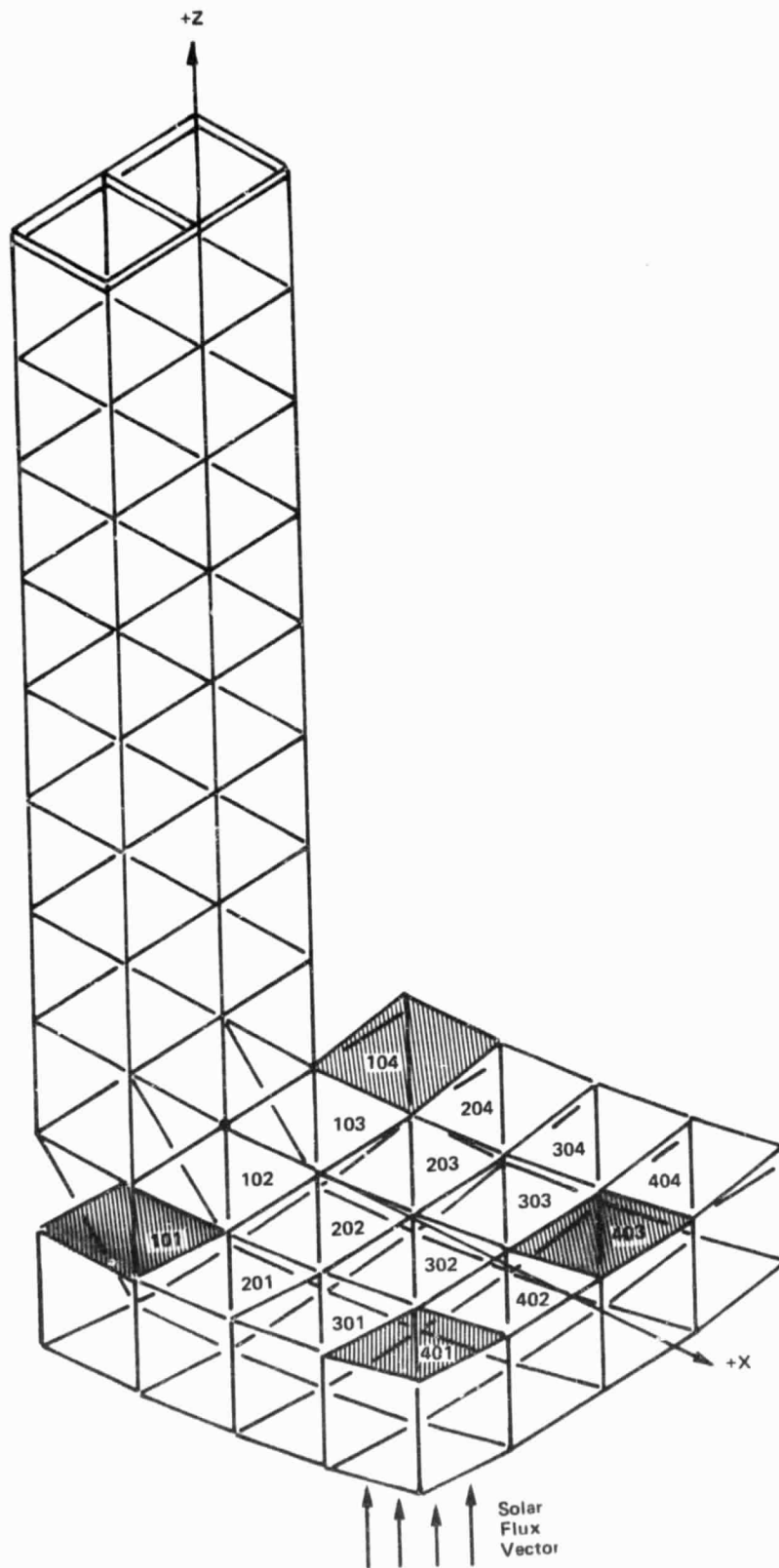


Figure 6 Typical Two-Dimensional Loading

2.1.4 Interpolation Limitations

The combination of choosing the analysis technique and the box sections to be analyzed, determine the resulting distorted reflector shape that will be used to solve the surface topography. The user should take care in making sure that the box sections, the interpolation technique, and the interpolation direction chosen will result in determining the correct distorted shape of the reflector. There are instances where none of the linear interpolation techniques can be used. As an example, the reflector in Figure 7 would have a cupped distorted shape (Fig. 7A), as a result of the solar flux vector shown. If box sections 103 and 503 were used to define the surface shape, linear interpolation would result in a reflector shape shown in Figure 7B. If box sections 103 and 303 were used to define the surface shape, linear interpolation would result in a reflector shown in Figure 7C. The solution to this problem is to define any two boxes for one dimensional interpolation and then define all remaining box sections as shadowed boxes. Although this is cumbersome and will increase the cost of the analysis, it will assure that the exact surface shape is determined.

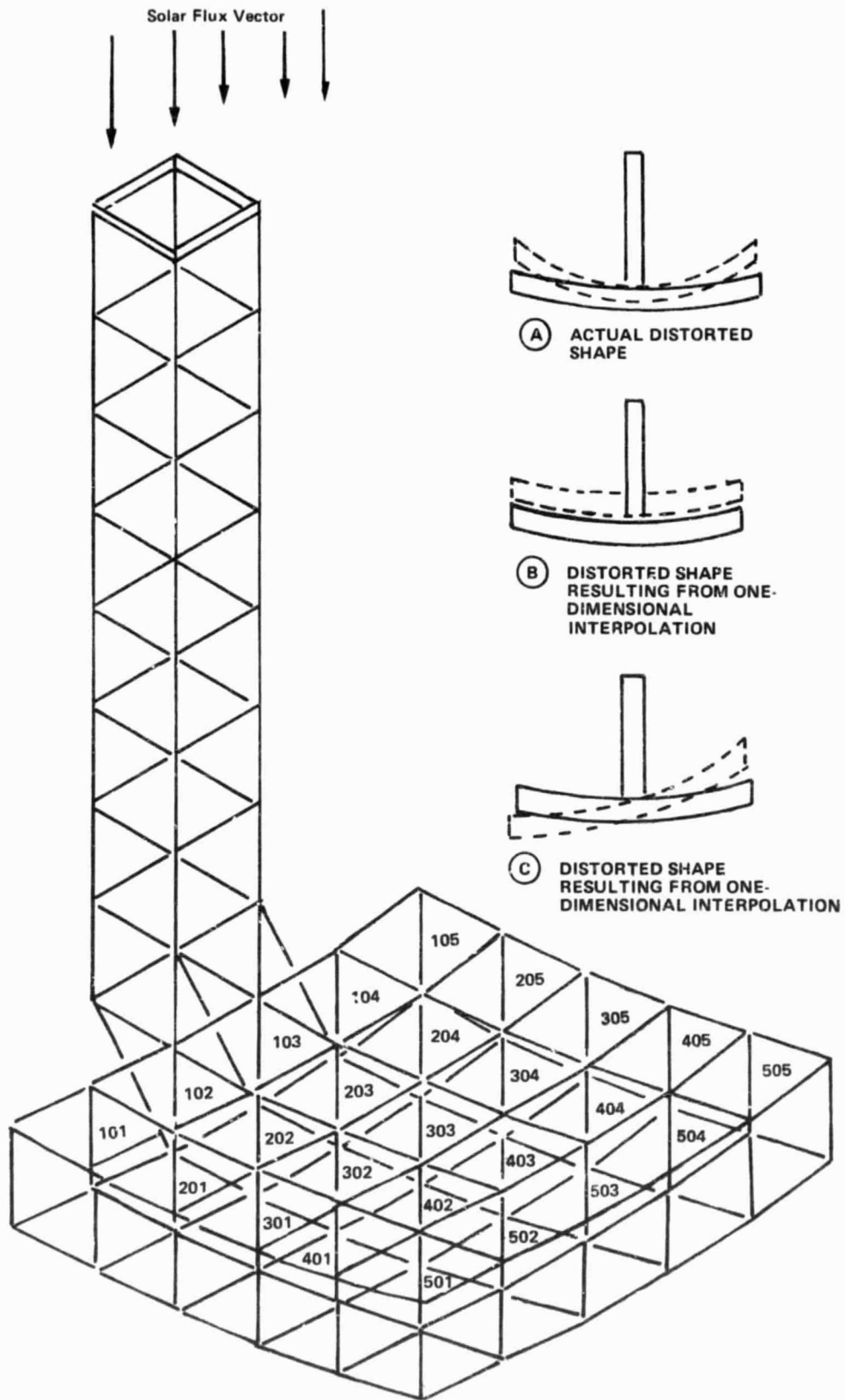


Figure 7 Typical Interpolation Limited Loading

2.2 TIE SPACING

The mesh tie system generator will request the user to input the nominal tie spacing to be used when generating the tie system design. The tie spacing chosen affects the magnitude of mesh pillowing. The mesh pillowing will in turn affect the rms surface distortion of the antenna and the resulting far-field pattern, antenna gain, and beam efficiency. Pillowing on mesh reflectors is caused by the mesh tie cords reacting against the biaxially tensioned mesh. In addition to the tie spacing, the magnitude of mesh pillowing is effected by the surface cord tension. However, the mesh tie system generator automatically calculates for the user the cord tension, for a given tie spacing, which will minimize the pillowing.

In choosing a nominal tie spacing the following equation can be used to estimate the resulting rms surface error for the antenna system.

$$[1] \quad \text{rms}(\text{pillow}) = \frac{0.05 \times \text{TS}^2}{F}$$

where

TS = tie spacing, m

F = antenna focal length, m, and

rms(pillow) = rms Surface error because of pillowing, m.

An acceptable rms surface distortion from pillowing is dependent on the other mechanisms causing surface distortions, i.e., manufacturing errors and operational environments. Therefore, the user should estimate an acceptable percent of the total allowable surface distortions resulting from pillowing. As an example, for radiometers, the allowable surface rms is considered to be 1/55 of a wavelength. Assuming the radiometer with a focal length of 120 meters is operating at 5.5 GHz, and 50% of the total allowable rms surface error is because of pillowing, then the allowable rms surface error because of pillowing equals 4.9×10^{-4} meters. From Equation 1, the tie spacing required, to assure that the rms surface error will not exceed the allowable, equals 1.09 meters.

2.3 MANUFACTURING TOLERANCE

Similarly to tie spacing, the mesh tie system model generator requires the user to input the manufacturing tolerance for tying the surface into shape. The input value will be used by the surface topography solver to randomly add to each tie point a manufacturing error and includes this error when solving for the total rms surface distortion. The manufacturing tolerance is used to define the 3σ value for a normal distribution curve of manufacturing errors. As with tie spacing, the magnitude of the manufacturing tolerance will affect the total rms surface distortion and the resulting far-field pattern, antenna gain, and beam efficiency.

In choosing a manufacturing tolerance, Equation 2 can be used to estimate the resulting rms surface error for the antenna system.

$$[2] \quad \text{rms}(\text{manf.}) = \text{MT}/3$$

where

MT = manufacturing tolerance, m, and
rms(manf.) = rms surface error because of manufacturing, m.

For the radiometer used above where 50% of total rms surface error is because of pillowing, 25% may be assigned to manufacturing, in which case the manufacturing tolerance would be 7.5×10^{-4} meters.

2.4 LIMITATIONS

Although the Integrated Mesh Analysis System has been created to solve most box truss reflectors, there are some instances when the analysis system will fail. Particularly when specifying large movements of the standoffs around any single tie system model. If the displacements defined in the loadcase generator cause the tie system to go slack, the model solver will terminate and printout the location where the singularity in the stiffness matrix occurred. If this should happen, it indicates that the box truss movement is too great and a reduction in the displacements is necessary.

As an example, assume a box truss antenna was analyzed using NASTRAN to determine the corner fitting distortions because of some thermal environment. These distortions were then applied onto the mesh tie system model. If the model solver fails to solve the tie system distortions because of a stiffness matrix singularity, this indicates that the thermal distortions of the box truss structure are too great and methods for reducing these distortions, (e.g., more thermally stable material used to build the truss) should be incorporated in the box truss design.

The mesh tie system model generator is the first of two interactive programs in the Integrated Mesh Analysis System. It is designed to create a mesh tie system design with minimum time and effort from the user. The user is required to input a few basic parameters to define the system. Varying these parameters enables the user to create any number of tie system designs within a short period of time. In addition, the mesh tie system model generator is used to generate the analytical tie system model and to determine additional parameters needed for the model solver, the surface topography solver, and the rf performance solver. The basic parameters include: (1) antenna diameter; (2) antenna focal length and/or radius; (3) the shape and number of box truss sections that make up the box truss support structure; (4) the surface interpolation technique to be used, Section 2.1; (5) the nominal tie spacing, Section 2.2; (6) the manufacturing tolerance level for tying the mesh surface, Section 2.3; (7) the frequency of operation for the antenna; (8) the feed horn type, i.e., regular or corrugated; and (9) the dB edge taper of the feed.

The mesh tie system model generator is capable of generating either a center fed or offset fed box truss circular aperture of either a spherical or paraboloidal reflector surface. The program is limited to creating a reflective surface of 25x25 box sections. To use the program's full capabilities, each box section must have an identical shape, i.e., either all rectangular or all square faces. However, if all the box sections are not identical, the model generator can still be used to create the tie system design for a single worst-case box section. In this case, the user will be required to input the coordinates of the standoff tops defining the box section.

Designing an antenna mesh tie system involves: (1) the determination of the ideal positions of the top of standoff points and the standoff heights for the entire box truss antenna surface; (2) the determination of the tie spacing for individual box sections of the reflector; (3) the creation of the detailed tie system design; and (4) the definition of sectional and material properties.

3.1 TOP OF STANDOFFS AND STANDOFF HEIGHTS

The standoff tops and standoff heights are generated by the program using the following four user defined parameters:

- 1) Reflector diameter;
- 2) Antenna focal length and/or radius;

- 3) Antenna type (i.e., center fed or offset fed);
- 4) Number of individual boxes in each direction.

The antenna type defines the origin of the coordinate system, with positive Z axis being in the direction of the focal point (Fig. 8 and 9). The reflector diameter limits the magnitude of X and Y coordinates. The focal length or radius defines the magnitude Z coordinate of the surface for a parabolic or spherical reflector, respectively. For a parabolic reflector, the Z coordinate for any X,Y pair is:

$$[3] \quad z = \frac{(X^2 + Y^2)}{4F}$$

For a spherical reflector, the Z coordinate for any X,Y pair is:

$$[4] \quad Z = R - \sqrt{R^2 - X^2 - Y^2}$$

Once the user has input the above parameters the program locates the tops of the standoffs in the following manner.

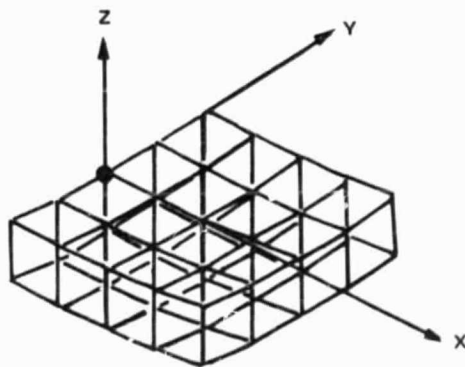


Figure 8 Coordinate System—Offset Fed Antenna

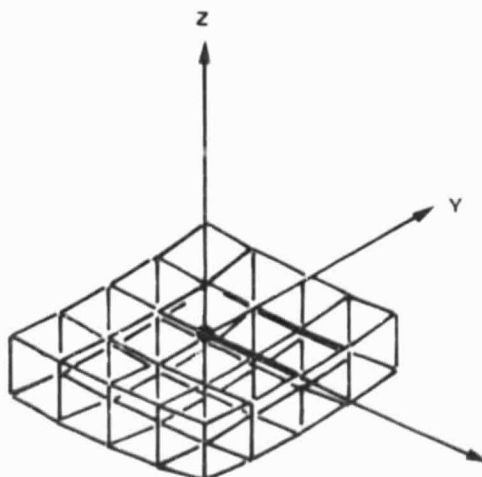


Figure 9 Coordinate System—Center Fed Antenna

First, surface cuts in the XZ and YZ planes are generated using the antenna focal length and the equation for a parabola. For the YZ plane cut, the vertex of the curve is always in the center, while for the XZ plane cut, the vertex of the curve will be either in the center, for a center-fed system, or at one end of the curve, for an offset-fed system.

Next, each curve is divided by straightline equidistant points, with the number of points being one greater than the defined number of individual box sections in that particular direction. Since the exact locations of these points cannot be solved with a closed form solution, they must be solved iteratively.

As an example, Figure 10 shows a curve in the XZ plane of an offset-fed system. The initial straight line distance between points, L_1 , is approximated to be D/NX , where D is the diameter and NX is the number of boxes in the X-direction. With the first point located at the vertex, Point 2 is located with its X-coordinate at L_1 . The Z-coordinate is found through Equation 5.

$$[5] \quad Z = \frac{X^2}{4F}$$

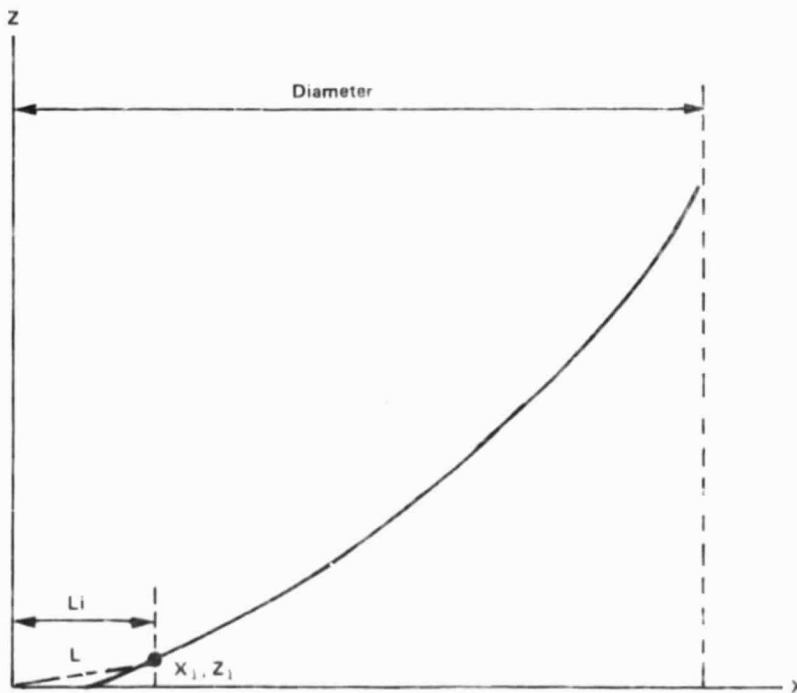


Figure 10 Cutaway-Offset Fed Antenna Location of Tops of Standoffs

The straightline distance between Points 1 and 2, L , is found through Equation 6.

$$[6] \quad L = \sqrt{(X_2 - X_1)^2 + (Y_2 - Y_1)^2}$$

This distance is compared to L_1 . If there is a difference, Point 2 is moved the difference, positively or negatively in the X-direction, e.g., if L is greater than L_1 , Point 2 is moved negatively by the distance $L-L_1$. A new Z-coordinate is found, along with a new L . A comparison is made again. This process continues until $L=L_1$. When the L is iterated to equal L_1 , Point 3 is located at an X-distance from Point 2 of L_1 . A Z-coordinate is calculated for Point 3 through Equation 5. The distance between Points 2 and 3, L , is found through Equation 7. L is compared to L_1 , and is iterated until it equals L_1 . This process goes on until the last point is located. Once this has occurred, a comparison between the X-coordinate of the final point, X_{fp} , and D is made. If X_{fp} differs from D , L_1 is increased or decreased by the difference divided by the number of boxes, NX , e.g., if $X_{fp} > D$, then L_1 (new) = L_1 (old) - $(X_{fp}-D)/NX$. The entire process begins again.

Once X_{fp} and D are equal, the same process is done for the YZ plane cut. The X-coordinates from the XZ curve and the Y-coordinates from the YZ curve are then used to form a grid of X,Y pairs. From the grid of X,Y pairs the Z-coordinates are found through Equations 1 or 2, resulting in the ideal position of each standoff top point. The program prints the coordinates and numbers each standoff point sequentially as shown in Figure 11. Also, the individual box sections are printed showing the corresponding standoff points that define the box section. The individual box sections have the following number scheme:

Row number in Y-direction times 100 plus the column number in the X-direction, Figure 11.

	1	2	3	4	5
5	101 7	102 8	103 9	104 10	
11	201 12	202 13	203 14	204 15	
16	301 17	302 18	303 19	304 20	
21	401 22	402 23	403 24	404 25	

Figure 11 Box Section and Tops of Standoffs Number Scheme

After the ideal position of each standoff top point has been printed, the program calculates the optimum standoff height. For a parabolic reflector, the optimum standoff height is a constant value defined by 2.0 times the distance between the top of the standoff and the intersection point between the slope of the paraboloid at point 5 and the vertical line from the standoff point for the outer most box section, (Fig. 12). For a spherical reflector, the optimum standoff height is calculated using the parabolic equation and then adjusted to meet the

spherical surface. On a spherical reflector, each standoff will vary in height. Since the user may have specific stowage requirements or may want to design a more stable tie system, the program allows the user to change the optimum standoff height. However, to assure a stable tie system, the program limits how small the standoff can be, i.e., 1.5 times the distance described above versus 2.0 times. Increasing the standoff height will produce a more stable tie system, however, packaging volume will increase. Decreasing the standoff height will reduce the tie system stability, however, packaging volume will decrease.

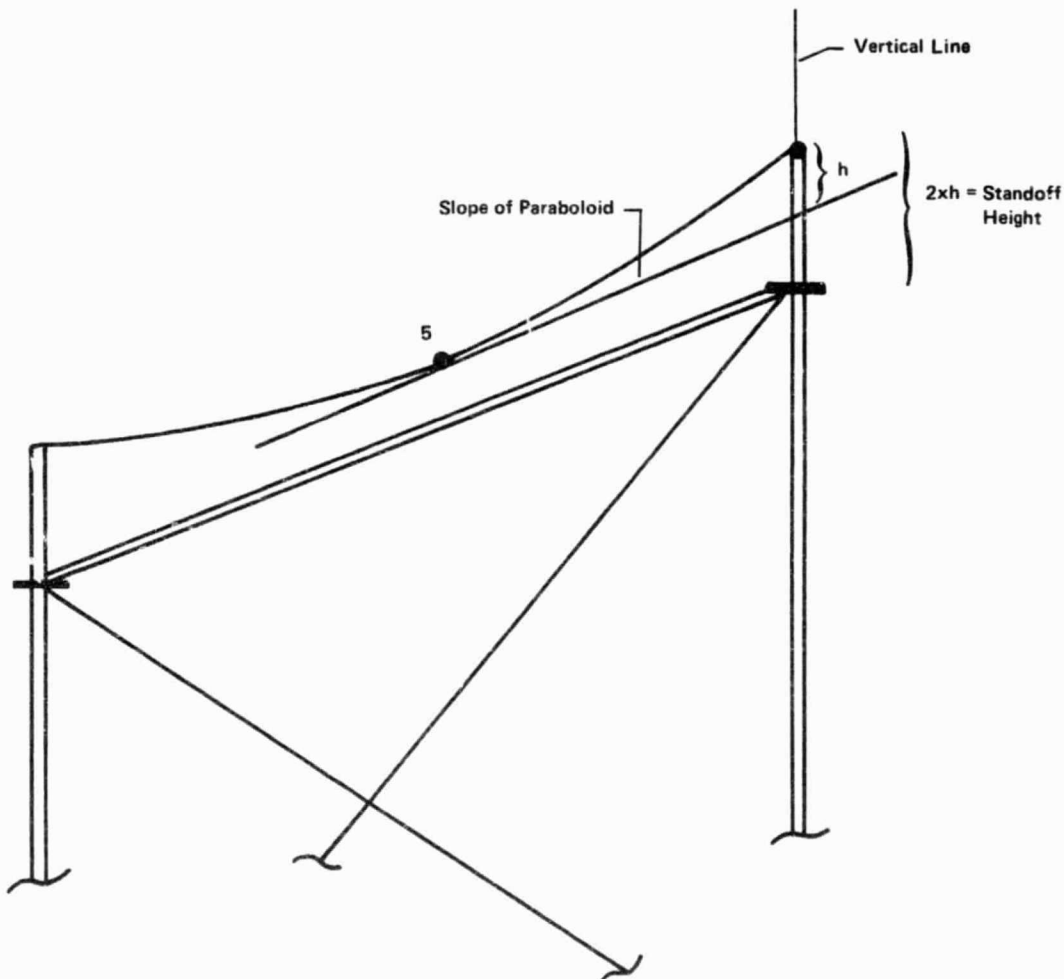


Figure 12 Standoff Height Determination

3.2 TIE SPACING

Once the location of the top of the standoffs and box sections have been printed, the program requires the user to specify the interpolation technique and the box section number(s) for tie system generation. The number of box section numbers input by the user depends on the interpolation technique chosen for the antenna system. In addition, the program will request the user to input the nominal tie spacing. However, before the tie system design can be generated, the user

defined tie spacing must be adjusted to ensure uniformity within all box sections. This is essential for one-dimensional and two-dimensional interpolation techniques and ensures a one-to-one correspondence between tie points from one box section to another. Figure 13 shows a cutaway section of a typical paraboloidal reflector.

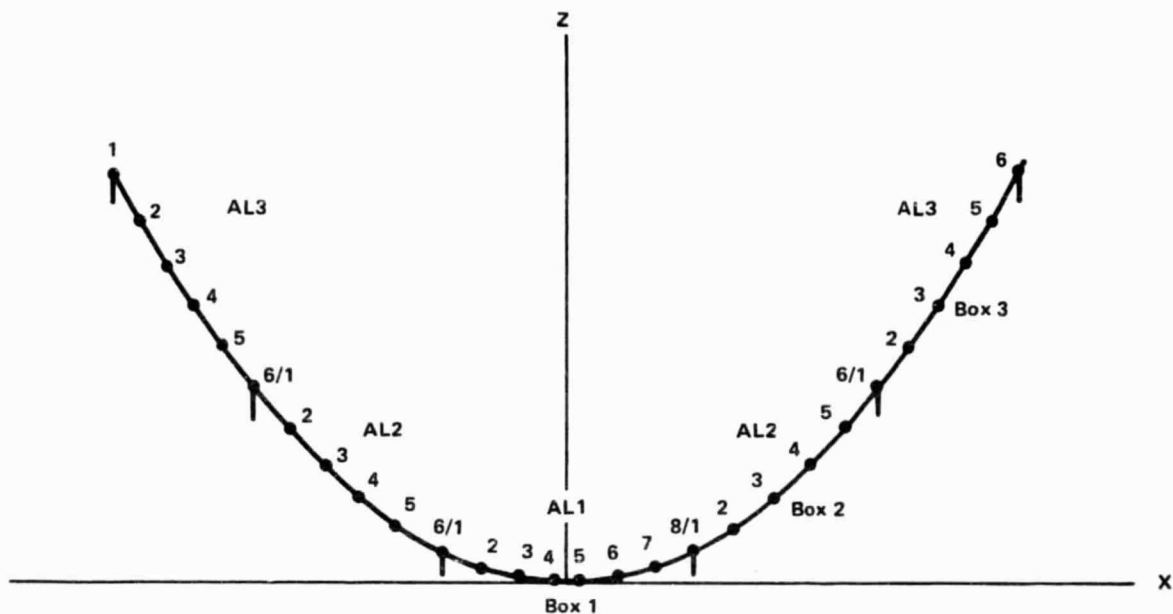


Figure 13 Cutaway Section of a Typical Paraboloidal Reflector

Note that the curvature increases as X approaches zero in either direction. Thus, while the standoff points are straightline equidistant from one another, the parabolic arcs that separate them vary in length with respect to their location from the origin, i.e., $AL1 > AL2 > AL3$. By using the same tie spacing for each box section, it is very likely to obtain different numbers of tie points per box section. Note that in Figure 13, AL1 has eight points, while AL3 has only six. This violates the one-to-one correspondence needed for interpolation.

To solve this problem, the nominal tie spacing is varied from box to box and from surface cord to surface cord, depending on the location of the box section with respect to the vertex of the reflector. For each surface cord in a particular box section, the tie spacing is found by multiplying the user specified tie spacing by the ratio of the arc length of the surface cord in question to the arc length of the corresponding surface cord in the box section closest to the vertex, Equation 7.

$$[7] \quad TS_n = \frac{TS \times AL_n}{AL_n}$$

where:

TS_n = Tie spacing of the surface cord;

TS = Tie spacing input by the user;

AL_n = Arc length of surface cord in question;

AL_v = Arc length of corresponding surface cord in the box section closest to vertex.

In Figure 13, the maximum tie spacing of the surface cord in Box 3 for one direction is as follows:

$$[8] \quad TS3 = \frac{TS \times AL3}{AL1}$$

This will yield eight tie points on AL3, so it has a one-to-one correspondence with AL1.

3.3 TIE SYSTEM

Once the tie spacing for each surface cord within a particular box section has been determined, the program will then generate the tie system design. The tie systems for each box are created in three parts:

- 1) Cross points and cross cords;
- 2) Radial tie points, surface cords and standoffs;
- 3) Tie-back cords.

3.3.1 Creation of Cross Points and Cross Cords

For each individual box section, the standoff tops are locally renumbered 1,2,3, and 4 while the bottom of the standoffs are locally renumbered 6,7,8, and 9 (Fig. 12). A fictional point 5 is created in the center of the box by bisecting the arc lengths in the X and Y directions. Tie point 10 is placed at the center of the arc between standoff points 1 and 2, i.e., its X-coordinate coincides with those of points 1 and 2, its Y-coordinate coincides with that of point 5. Similarly, tie point 15 is placed at the center of the arc between standoff points 1 and 3, i.e., its X-coordinate coincides with the X-coordinate of point 5, its Y-coordinate coincides with those of points 1 and 3. The placements of points 5, 10, and 15 are shown in Figure 14.

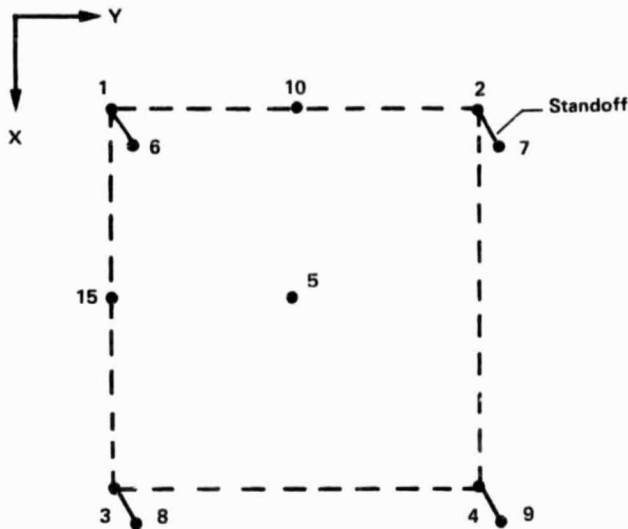


Figure 14 Renumbering of Standoffs

Cross points are placed on the arc in between points 10 and 5. These cross points are spaced from one another at a distance of no farther than the adjusted tie spacing. The final point, i.e., the cross point closest to point 5, may not be farther away from point 5 than one-half of the adjusted tie spacing. These points are numbered in increments of 10 from point 10 to point 5, e.g., point 20 and 30 (Fig. 15). On the other side, cross points are placed in the same fashion starting with a cross point that is placed at the center of the arc between standoff points 3 and 4. On the arc between this point and point 5, cross points are placed at no farther from one another than the adjusted tie spacing. Once again, the point placed closest to point 5 may not be farther away than one-half tie spacing, e.g., point 40. The numbering continues in increments of 10. In the Y-direction, cross points are placed in the same fashion, numbered from 15 in increments of 10 (Fig. 15).

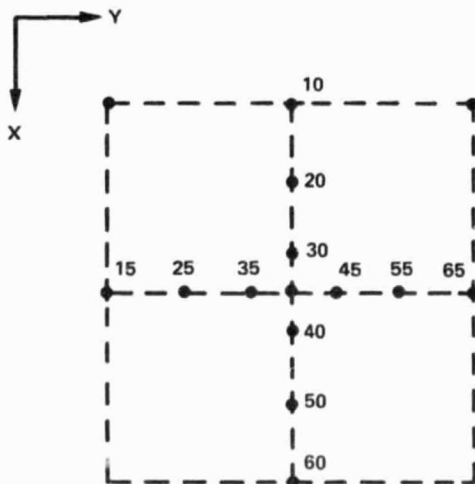


Figure 15 Creation of Cross Points

Once the cross points have been defined, cross cord segments are placed between each cross point as shown in Figure 16. The cross cords are numbered consecutively starting at 100 in the X-direction and 200 in the Y-direction, Figure 16. Note that the outermost cross cord points, e.g., points 10 and 20, are not connected by a cross cords.

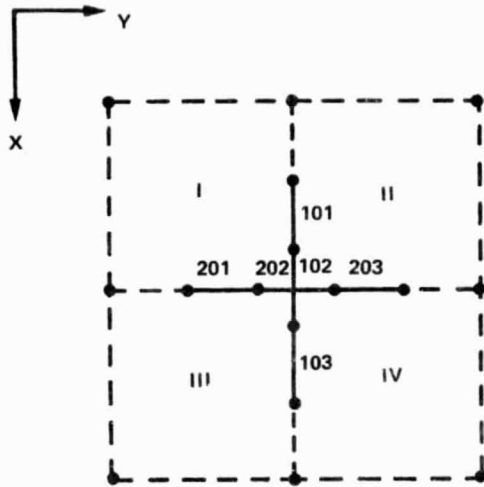


Figure 16 Creation of Cross Cords

3.3.2 Creation of Radial Tie Points and Surface Cords

With the placement of cross cords, the box is now divided into four distinct quadrants, numbered I, II, III, and IV in conjunction with their standoff number (Fig. 16). Each quadrant has its own standoff and cross points that define its borders. On an arc from each standoff to each cross point, radial tie points are generated at equal spacing. The spacing is equal to the adjusted tie spacing except for the final tie point that is placed halfway between the previously placed point and the cross point. This is to ensure that the cross points and the radial points are not unreasonably close together. The numbering scheme for these radial points is the quadrant number times 10,000 plus the cross point number times 10 plus the sequential number of the tie point from the standoff, Figure 17.

Next, radial surface cord segments are placed from the standoff to each cross point, via the radial tie points (Fig. 18). The numbering scheme for these cord segments is the quadrant number times 10,000 plus the cross point number times 10 plus the sequential number of the cord segment from the standoff.

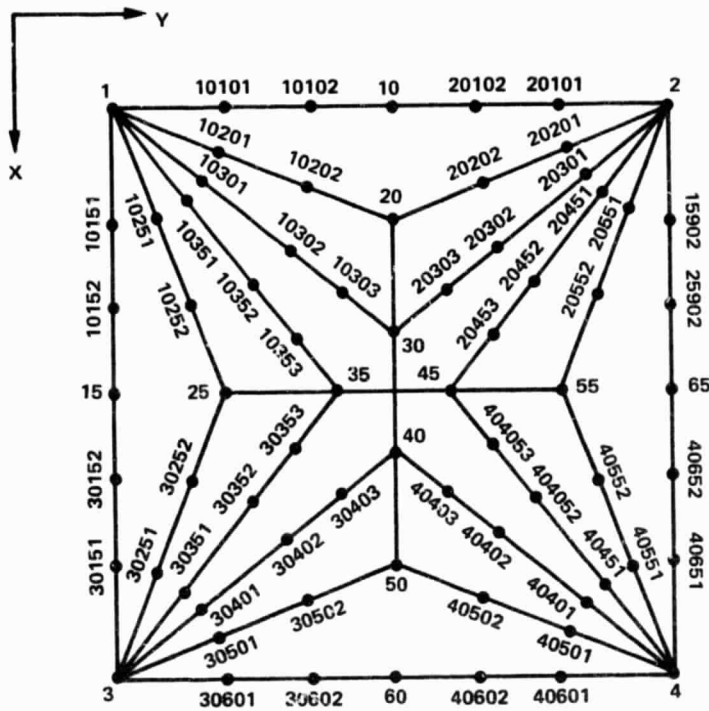


Figure 17 Tie Point Numbering Scheme

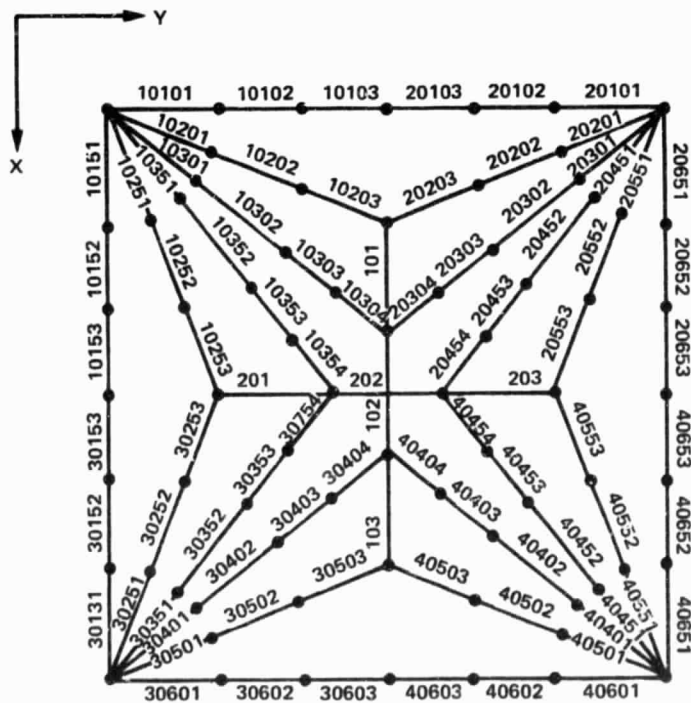


Figure 18 Surface Cord Numbering Scheme

3.3.3 Creation of Tieback Cords

After the surface tie points have been determined, each tie point is connected to their corresponding bottom of standoff by a tieback cord, i.e., the surface points in quadrant I, including those cross points that border quadrant I, are connected by tieback cords to the bottom of the standoff of quadrant I, point 6 (Fig. 14). For cross points, since they all border on two quadrants, this means that they are connected to two standoffs.

3.4 ELEMENT SECTIONAL AND MATERIAL PROPERTIES

The tie system design process is completed with the inclusion of sectional and material properties. The three distinct types of structural elements in the mesh tie system are as follows:

- 1) Cross cord and surface cords,
- 2) Tieback cords,
- 3) Standoffs.

For the surface and tieback cords, the user is afforded the convenience of choosing either graphite, quartz, or some other material. For graphite and quartz, all relevant material properties are furnished by the program. These values are given in Table 4.

Should the user opt for other materials, the above type of data will be required from the user.

*Table 4
Material Properties for Graphite and Quartz Cords*

	Graphite	Quartz
Modulus (Pascals)	2.34E11	6.89E10
Density (kg/cu, m)	1770	2200
CTE (m/m/°C)	-0.40E-6	-0.54E-6

For the standoff, the user must furnish the above type of data and, additionally, the shear modulus and Poisson's ratio.

Since tie cords have axial stiffness only, the only pertinent sectional property, which the user must input, is the cross-sectional area.

The standoff is a three-dimensional beam element. Therefore, it is capable of six degrees of freedom at each end. The user is asked for the following sectional properties:

- 1) Cross-sectional area,
- 2) Moment of inertia about Local Y-axis,
- 3) Moment of inertia about Local Z-axis,
- 4) Extreme fiber distance from Local Y neutral axis,
- 5) Extreme fiber distance from Local Z neutral axis.

Figure 19 defines the local coordinate system of the standoff in relation to the global axes. Note that Local Y is parallel to Global Y and that Local Z is parallel to Global X.

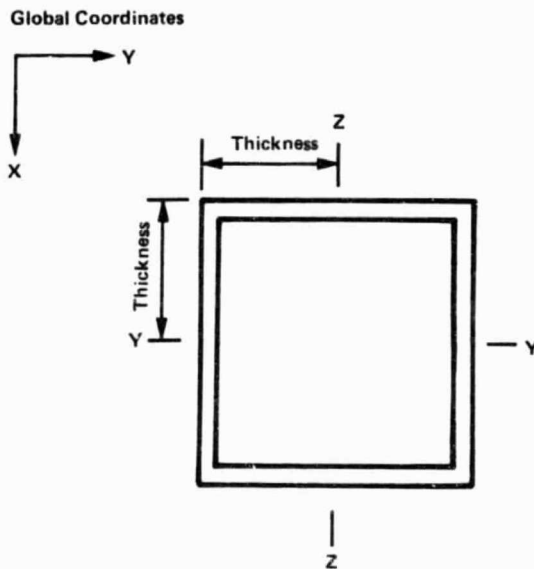


Figure 19 Standoff Cross Section

3.5 TIE SYSTEM ANALYTICAL MODEL

In addition to the tie system design, a tie system analytical model is generated for each box section. The tie system analytical model is a finite-element model representing the tie system design. Tops and bottoms of standoffs and tie points are represented as nodes, while the standoffs, surface cord, cross cord, and tieback cord segments are represented as elements. Depending on the number of tie points, the full tie system design created earlier may or may not be used for finite element analysis. Because of limited computer memory, the finite element model is limited to 145 node points. Also, since the time and expense of analysis is directly related to the size of the model, one may choose to reduce the tie system design further without suffering any significant loss of accuracy. An example of such a reduction will be discussed later.

The program reduces the tie system design by increasing the tie spacing and the cross-sectional areas of the tie cords. The tie spacing for the analytical model is found by dividing the tie spacing of the tie design by the square root of the model percentage desired. For example, if a 65% model is desired, the tie spacing is divided by the square root of 0.65. This reduces the number of nodes to roughly 65% of the original number of tie points. This is true because the relationship between the increase in tie spacing and the reduction of the number of nodes is approximately a square function. By increasing the tie spacing, the number of cross nodes is directly reduced, and with that reduction, the number of radial surface cords is reduced. The nodes on the remaining radial surface cords have their spacings increased, further reducing the number of nodes. The cross-sectional areas of the elements representing the tieback cords and radial surface cords are increased to ensure that the finite-element model will have the same effective stiffness as the original tie system design. For elements representing tieback cords, the cross-sectional area is determined by:

$$[9] \quad ATBR = ATBI/res$$

where

ATBR = area of tieback element reduced model,
ATBI = area of tieback cord initial design,
res = fraction of model desired for analysis.

For element representing the surface cords, the cross-sectional area is determined by:

$$[10] \quad ARSCR = ARSCI/res$$

where

ARSCR = area of surface element reduced model
ARSCI = area of radial surface cord initial design
res = fraction of model desired for analysis

However, there is a limit, to the amount of reduction that can take place. The program will determine this amount, based solely upon having a workable configuration. This will ensure that there is at least one tie point between each standoff and its corresponding cross points on every radial surface cord, i.e., no standoff will be connected directly to a cross point.

In the finite-element model, the nodes are numbered in the same fashion as the tie points, while the standoff elements are numbered 1 thru 4, and the surface and tieback cord segments are numbered sequentially from 5.

3.5.1 Reduced Analytical Model Accuracy

To show the accuracy and effectiveness of reducing the full tie system design for the analytical model, a sample problem was run for both a full tie system design and a 30% analytical model of the same tie system. A 1-g gravity environment was applied on both models. The sample problem used the tie system design for a 4.572 meter (15 ft) box section with a nominal tie spacing of 0.508 meters (20 in.). Table 5 shows the parameters used to design the tie system along with the resulting size of both models. Note, the full size tie system model is larger than allowed. However, special provisions were made to allow this larger size to be run within the model solver.

Table 5 Design Parameters and Model Size

	Full-Size Model	30% Analytical Model
Reflector Diameter, m	4.572	4.572
Reflector Focal Length, m	9.144	9.144
Number of Box Sections	1	1
Tie Spacing, m	0.508	0.9275
Standoff Height, m	0.5715	0.5715
Nodes (Tie Points)	212	68
Elements (Tie Cord Segments)	482	170

Comparison of both runs showed the 30% analytical model closely matched the behavior of the full tie system model under the gravity environment. Table 6 shows the results of each model and the percent of error between the two runs. Another significant result, one that shows the effectiveness of reducing the model, was the cost savings when using the reduced model. Using the Cyber 750 to run each model, the full tie system model used approximately 400 seconds of execution time, versus 28 second for the reduced model, a reduction in execution time of 14 times.

Table 6 Finite Element Results

	Full-Size Model	30 % Analytical Model	% Error
Total Mass at 1-g, kg	1.53	1.49	2.5
Reaction Force, N	11.37	10.55	7.2
Maximum Tie Point Displacement Along a Surface Cord, m	-3.67×10^{-4}	-3.88×10^{-4}	5-20
Maximum Tie Point Displacement Along a Cross Cord, m	-5.42×10^{-4}	-6.84×10^{-4}	
Maximum Tie Cord Strain	1.02×10^{-3}	0.947×10^{-3}	7.0

3.6 DETERMINATION OF INITIAL STRAIN

The pretension condition is the actual tension in each tie cord resulting from tying the surface into shape. To solve the pretension condition of the mesh tie system, the model solver requires an initial strain value for the corner surface cord elements attached directly to the standoffs, e.g., 10101, 20451, and 40501 (Fig. 20). How these strain levels are used by the model solver is discussed in Section 6.1.

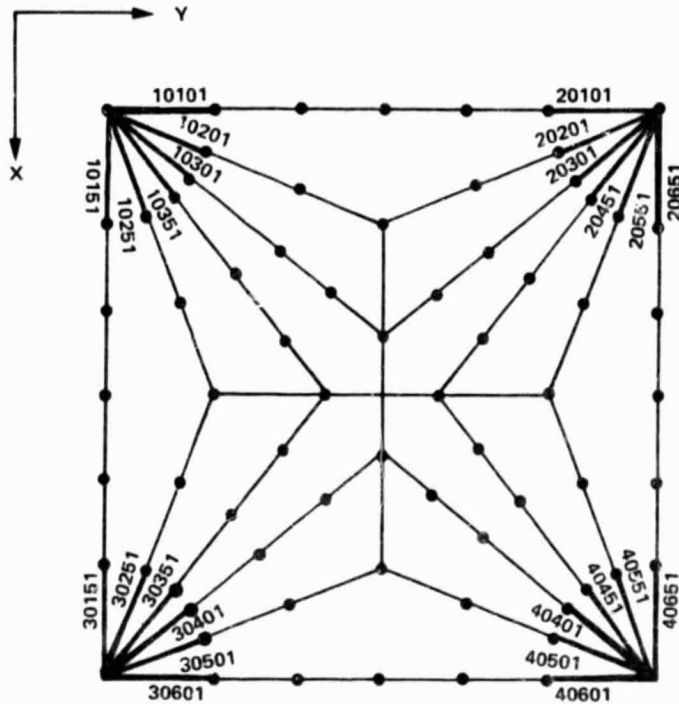


Figure 20 Initially Strained Cords

To determine the corner strain value, the average strain in the surface cords is first determined. This average strain includes the base strain and the additional strain because of any operating load condition such as imposed by temperature changes from the initial condition.

The base initial strain, ϵ_B , Equation 11, is derived from the fact that the tie system reacts the biaxial tension field in the mesh.

$$[11] \quad \epsilon_B = \frac{2 \times 1.78 \times TS}{A \times E}$$

where

- A = the user input area of the surface cords,
- E = modulus of elasticity,
- TS = user defined tie spacing,
- 1.78 = mesh biaxial tension field, N/m.

The mesh tension field of 1.78 N per meter is the minimum tension required to produce a flat reflective surface by removing any wrinkles in the mesh caused by stowage condition. The two times factor is the result that pillowing is minimized when the surface cord tension is twice that of the mesh tension field.

The additional strain because of operating load conditions is obtained through the use of temperature. The user is asked for the greatest change in temperature, ΔT_{max} . If the user is creating a tie system design to withstand gravity or pressure loading, an equivalent T_{max} should be used to assure the tie system will not go slack during the loading condition. Using the ΔT_{max} , two strains are calculated, the maximum of which is added to the base strain. The first strain is the thermal strain in the surface cords, Equation 12. The second is the thermal strain in the tieback cords, Equation 13.

$$[12] \quad \epsilon_{TSC} = \Delta T_{max} \times CTE_{sc}$$

$$[13] \quad \epsilon_{TTB} = \Delta T_{max} \times CTE_{tb} \times L_{tb}/L_{sc}$$

where

ϵ_{TSC} = temperature strain of surface cords,
 ϵ_{TTB} = temperature strain of tieback cords,
 CTE_{sc} = CTE of the surface cords,
 CTE_{tb} = CTE of the tieback cords,
 L_{tb} = length of the longest tieback,
 L_{sc} = length of the longest surface cord.

By assuming that any temperature change is in the worst direction, i.e., the cord lengthens, these equations are used to approximate the relaxation of strain caused by a change in temperature. Increasing the base initial strain in each cord by this amount will assure that during the worst-case loading environment, the cord tension will never go below the base strain, ϵ_B .

After the average initial strain is determined, the value is multiplied by the number of surface cord segments, NSC, between the standoff and cross cord. The result is the value to be input as the initial strain at the corner surface cord elements, Equation 14.

$$[14] \quad \epsilon_I = NSC \times (\max [\epsilon_{TSC}, \epsilon_{TTB}] + \epsilon_B)$$

where:

NSC = Number of surface cords to the crosscord,
 ϵ_I = Total initial strain,
 ϵ_B = Base strain from Equation 12,
 ϵ_{TSC} = Temperature strain from Equation 13,
 ϵ_{TTB} = Temperature strain from Equation 14.

Multiplying the average initial strain by the number of surface cord segments assures that when the strain in the corner surface cord segment is distributed along the length of the surface cord, the average strain is approximately equal to the calculated average strain. In Figure 18, the initial strain, ϵI , put on cord 10101 is three times the combined strain, since there are three cord segments between the stand-off and the cross cord in that line. The initial strain, ϵI , put on cord 10301 is four times the combined strain, since there are four cord segments between the standoff and crosscord in that line.

4.0 LOAD GENERATOR

This load generator is the second of two interactive programs in this package. It is designed to convert user input on load conditions into an input deck for use in the model solver. Load conditions are input by the user for each box earmarked for analysis, including shadowed boxes, for any number of loadcases.

For each loadcase, there is a choice of two loadtypes. A Type 0 loadcase allows the user to create new nodal point loads, constraints, pressure and gravity loads, and temperatures. A Type 1 loadcase makes use of the information in previous loadcase, while amending only the temperatures.

The program allows the user to create loadcases define the following conditions:

- 1) Nodal point loads,
- 2) Nodal constraints,
- 3) Pressure loads,
- 4) g-loads,
- 5) Element temperatures.

4.1 NODAL LOADS

This section of the program enables the user to place point loads on any node in any of six directions. The user will be asked for the node number, the force value, and in which directions the force acts. If there is more than one force acting on the node, the user will again be asked for the force values and its corresponding directions. If, as is often the case, there are many nodes with identical point loading patterns, the user will be asked to name those nodes, so that the program may duplicate the loads.

The specification of directions is done numerically as follows:

Force in the X-direction--1,
Force in the Y-direction--2,
Force in the Z-direction--3,
Moment about the X-axis--4,
Moment about the Y-axis--5,
Moment about the Z-axis--6.

The sign attached to the force value signifies that the force acts either positively or negatively, e.g., a 10 N force in the negative Y-direction is represented by a user input force value of -10 N in direction 2.

4.2 NODAL CONSTRAINTS

This section works in much the same way as the nodal loads section. The user is asked for the node number, any initial displacement value, and the directions in which it is displaced. The directions are once again specified numerically, in the same fashion as shown in the Nodal Loads section.

Displace and hold in the X-direction--1,
Displace and hold in the Y-direction--2,
Displace and hold in the Z-direction--3,
Rotate and hold about the X-axis--4,
Rotate and hold about the Y-axis--5,
Rotate and hold about the Z-axis--6.

The specified nodes are held at the specified displacements and corresponding directions. If a node is to be constrained, i.e., without being displaced, the user must input an initial displacement of 0.0.

Since nodes 6, 7, 8, and 9 represent the corner fittings of the box truss, and the assumption is that the truss structure is infinitely stiffer than the tie system, the loadcase generator automatically holds these nodes in all directions at an initial displacement of 0.0. However, to input box truss distortions onto the tie system model, the user may override the zero displacement by specifying a displacement other than zero for these nodes in the X, Y, and Z translation directions. The user may not specify rotations at these nodes because of the fact that the tops of the standoffs, i.e., nodes 1, 2, 3, and 4 are held in the X and Y direction approximates the effect of having adjacent box tie systems with similar loads reacting at the tops of the standoffs.

4.3 PRESSURE AND G-LOADS

The user is asked for pressure loads in Global X, Y, and Z directions. These are input in units of N/m^2 .

The user is asked for gravity loads in Global X, Y, and Z directions. These are input in units of m/s^2 , e.g., a 1-g load is input as 9.81 m/s^2 .

4.4 TEMPERATURES

The user is asked for the temperatures and a range of elements to which it applies, e.g., a 100°C temperature from element 5 to 82. This means that each element from 5 to 82, inclusive, is at 100°. The user is also asked for a reference temperature. The reference temperature is the base temperature from which the changes in temperature are calculated, e.g., if an element has a temperature of 100° and the reference temperature is 70°, the change in temperature is 30°. If an element has not been assigned a temperature, its temperature is assumed to be the reference temperature.

The model optimizer program was created to increase the efficiency of the model solver. Primarily this program is used to minimize the nodal bandwidth of the finite-element models. The reduction in bandwidth decreases the solution time and dramatically decreases the size of computer core needed to solve the finite-element problem. It also allows the mesh tie system generator to create node numbers that are convenient to the user, i.e., node numbers that define the particular quadrant and location within the quadrant for each tie-point in the box section, without affecting the bandwidth size of the finite-element model.

The model optimizer uses a bandwidth reduction technique created by Mr. R. J. Collins, Stearns-Rogers, Inc*. This optimization technique was chosen over other techniques because it produces the smallest bandwidth in the least execution time. In general, this technique will reduce the original bandwidth by over 60%. Because tie system requirements, the program was modified to allow up to 100 surface cords and 100 tieback cords to be attached to any one standoff, and still take advantage of the fact that a maximum of six tie cords are attached to any single internal tie point. This reduced the core requirements and decreased the solution time even further for optimizing the tie system. Using this method, the tie system model node numbers are automatically renumbered in such a way as to minimize the nodal bandwidth. This renumbering is invisible to the user, and a special program matrix is created that allows the model solver to convert the renumbered nodes back to the original node numbers.

An illustration of how the bandwidth is reduced is shown in Figures 21 and 22. Figure 21 graphically shows an interconnectivity matrix for a typical tie system model consisting of 32 node points, resulting in a nodal bandwidth of 32. Figure 22 shows the same tie system model after renumbering the nodes through the optimizer. The optimized nodal bandwidth equals 11, a 65% reduction from the original bandwidth.

*R. J. Collins: "Bandwidth Reduction by Automatic Renumbering."
International Journal for Numerical Methods in Engineering, Vol 6, pp
345-356, 1973.

Node	1	2	3	4	10	20	30	40	15	25	35	45	10101	10201	10151	10251	20101	20201	20351	20451	30301	30401	30151	30251	40301	40401	40351	40451	6	7	8	9			
1	X												X	X	X	X															X				
2		X																X	X	X	X											X			
3			X																			X	X	X	X								X		
4				X																					X	X			X				X		
10					X								X				X													X	X				
20						X	X							X				X												X	X				
30						X	X															X			X							X	X		
40								X														X				X						X	X		
15									X							X								X						X	X				
25										X	X						X								X					X	X				
35										X	X									X											X	X			
45													X								X								X	X	X				
10101	X				X								X																	X					
10201	X					X								X																					
10151	X							X							X																				
10251	X								X							X																			
20101		X			X												X																		
20201		X				X												X																	
20351		X								X									X																
20451		X										X								X															
30301			X				X															X													
30401			X				X																X												
30151			X					X																X											
30251			X						X																X										
40301				X			X																			X									
40401				X			X																				X								
40351				X						X																			X						
40451				X								X																		X					
6	X				X	X			X	X			X																		X				
7		X			X	X					X	X																				X			
8			X			X	X	X	X																								X		
9				X		X	X			X	X																							X	

Figure 21 Typical Unoptimized Interconnectivity Matrix

Node	10101	1	10	6	10201	10151	10251	20101	7	20	15	25	2	35	45	20201	20351	20451	30	30151	8	30251	40351	9	40451	30301	40301	3	40	30401	4	40401	
10101	X	X	X	X																													
1	X	X	X	X	X	X	X																										
10	X		X	X				X	X																								
6	X	X	X	X	X	X	X			X	X	X																					
10201		X		X	X					X																							
10151		X		X		X					X																						
10251		X		X			X					X																					
20101			X					X	X				X																				
7			X					X	X	X			X	X	X	X	X	X															
20				X				X	X							X			X														
15					X					X										X	X												
25						X					X	X								X	X												
2								X	X			X				X	X	X															
35								X		X		X				X							X	X									
45								X							X		X							X	X								
20201								X	X		X					X																	
20351								X			X	X					X																
20451								X			X	X					X																
30									X										X	X		X		X	X	X	X	X					
30151										X										X	X								X				
8										X	X								X	X	X	X				X	X	X	X				
30251										X											X	X							X				
40351												X											X	X								X	
9												X	X					X					X	X	X	X	X	X	X	X	X	X	X
40451															X									X	X							X	
30301																			X		X					X	X						
40301																			X				X			X	X					X	
3																				X	X	X				X	X	X	X				
40																						X		X					X	X	X	X	X
30401																					X						X	X	X				
4																							X	X	X	X	X	X	X	X	X	X	X
40401																								X				X	X	X	X	X	X

Figure 22 Typical Optimized Interconnectivity Matrix

In addition to minimizing the tie system nodal bandwidth, the Model Optimizer is used to produce the three input files necessary for the Model Solver. The first file defines the nodal connectivity, as well as the length, directional cosines, sectional and material properties for each element in the model. Also written to this file is the effective mesh area and area ratios used for pressure loading on the model. The methodology for determining the effective area and area ratios is discussed in Section 6.3. The next file created is the renumbered node matrix, used by the model solver to convert the renumbered nodes back to the original numbers. The final file is the first section of the users output file from the finite-element solution. This file shows: (1) the nodal point geometry, (2) the element connectivity, (3) the element properties, (4) material properties, and (5) the results of the bandwidth reduction. This file is written to provide the user with a checkpoint in a readable form, to ensure that the desirable model properties were input correctly before solving the model.

The finite-element model solver uses a banded matrix solution technique combined with nonlinear stress-stiffening and nonlinear cable elements. The cable elements are used to represent the mesh tie cords, i.e., the cable element is a tension-only member. This program is unique in that it has been written specifically for the tie system models, thereby streamlining both solution time and iterations needed to solve the model. In addition, the pretension condition is automatically determined by the model solver. The model solver is capable of solving tie system distortions resulting from the following conditions:

- 1) Nodal point loads,
- 2) Specified displacements at nodes,
- 3) Global pressure loads,
- 4) Global g-loading,
- 5) Element temperature changes.

Although the model solver uses conventional finite-element techniques to solve the tie system distortions, loads and reactions, there are a few unique features that have been incorporated because of tie system specific requirements. The following describes in detail these various unique features.

6.1 PRETENSION CONDITION

The pretension condition is the actual tension in each tie cord resulting from tying the surface into shape. To solve the pretension condition, the model solver calculates the strain in each cord using ten single-step iterations. These iterations are invisible to the user and only the final "pretensioned condition" is printed out by the program.

For the first two iterations, the initial strain is input from what was previously calculated by the model generator. This initial strain level assures that any following user defined loadcases will not cause the ties system to go slack. This is accomplished by requiring the user to input the equivalent maximum temperature change that the tie system will experience. The model generator determines the proper initial strain by not only using the maximum temperature change but also the surface cord and tieback cord material data and assumed mesh tension field of 1.78 N per meter; Section 3.6 discusses the details of this process. The model solver takes this initial strain and applies it to

only those cords that are directly attached to a standoff, e.g., cord 10151, 10101, and 20301 in Figure 20. The result after two iterations is a set of cord strains for the entire system. These cord strains are then used by the next single step iteration as the initial strain condition. The displacements on the model are reset to zero and the solution process is started over. This same process is continued for the remaining single-step iterations. The results after the ten iterations is a pretensioned tie system model that closely approximates the required tie system geometry, i.e., the resulting nodal displacements are near zero. Only after the model solver has completed the pretensioned condition, are the user's defined loadcases applied to the model.

6.2 NONLINEAR EFFECTS

The model solver incorporates two forms of nonlinear analysis techniques. The first, stress-stiffening, is an effect that causes a stiffness change in the element because of the loading or stress within the element. This effect is more predominate in thin, highly stressed structural elements (e.g., tie cords), therefore, only the tie cords are stress stiffened. The standoffs represented by beam elements are conventional linear elements. The second nonlinear effect is the use of cable elements (tension-only members) to represent the tie cords. If a tie cord goes slack, the element is removed from the global stiffness matrix of the model.

For a cable member, the following derivation of the stiffness matrix (including stress-stiffening) was developed for the model solver.

A cable element between nodes i and j, Figure 23, which experiences both axial and lateral deflections, u_i , v_j , u_j , and v_j , has the following equation for the axial strain (ϵ) in the cable:

$$[15] \quad \epsilon_x = \epsilon_u + \epsilon_v$$

where

$$\epsilon_u = (U_i - U_j)/L,$$

$$\epsilon_v = 1/2[(V_j - V_i)/L]^2.$$

The strain energy (U) in the element is defined by:

$$[16] \quad U = AEL \epsilon_x^2 / 2$$

where

A = Area of member,
 E = Modulus of elasticity,
 L = Length of member.

Substituting Equation 15 into the above equation results in:

$$[17] \quad U = AEL \epsilon_u^2 / 2 + PL\epsilon_v$$

where

P = AE ϵ_u = axial member force.

Assuming small displacement theory, the ϵ_u^2 can be assumed to be zero. Expressing ϵ_u and ϵ_v into matrix notation results in:

$$[18] \quad \epsilon_u = 1/L [-1 \ 1] \{U \ U\}, \quad \epsilon_v = 1/2L - \begin{Bmatrix} v_1 \\ v_j \end{Bmatrix}^T [-1 \ 1] [-1 \ 1] \begin{Bmatrix} v_1 \\ v_j \end{Bmatrix} .$$

Substituting ϵ_u and ϵ_v into the strain energy equation and expanding to a three-dimensional problem results in:

$$[19] \quad U = \frac{1}{2} \{d\}^T \frac{AE}{L} \begin{bmatrix} 1 & 0 & 0 & -1 & 0 & 0 \\ 0 & 0 & 0 & 0 & 0 & 0 \\ 0 & 0 & 0 & 0 & 0 & 0 \\ -1 & 0 & 0 & -1 & 0 & 0 \\ 0 & 0 & 0 & 0 & 0 & 0 \\ 0 & 0 & 0 & 0 & 0 & 0 \end{bmatrix} + \frac{P}{L} \begin{bmatrix} 0 & 0 & 0 & 0 & 0 & 0 \\ 0 & 1 & 0 & 0 & -1 & 0 \\ 0 & 0 & 1 & 0 & 0 & -1 \\ 0 & 0 & 0 & 0 & 0 & 0 \\ 0 & -1 & 0 & 0 & 1 & 0 \\ 0 & 0 & -1 & 0 & 0 & 1 \end{bmatrix} \{d\}$$

The first 6x6 matrix is the conventional stiffness matrix, [k], where the second matrix is the stress-stiffening matrix. The combined stiffness matrix is transformed into the global coordinates by the standard transformation matrix [T], of directional cosines.

$$[20] \quad [K] = [T]^T [k] [T].$$

Because of these nonlinear techniques, the model must be solved iteratively. The flow chart for this process is shown in Figure 24. The solution for the nonlinear problem is based on the Newton-Raphson method, which uses a piecewise linear solution scheme based on Equation 21.

$$[21] \quad [K] \{ \Delta D_{i+1} \} = \{ R \} - \Sigma [k] \{ d \}$$

$\{ d \}$ = Displacements in member coordinate system,
 $\{ \Delta D \}$ = Displacements in global coordinate system,
 $\{ R \}$ = Force vector.

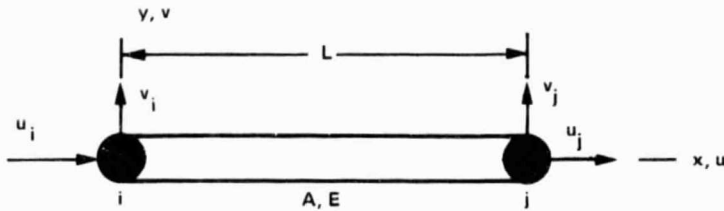


Figure 23 Typical Cable Element

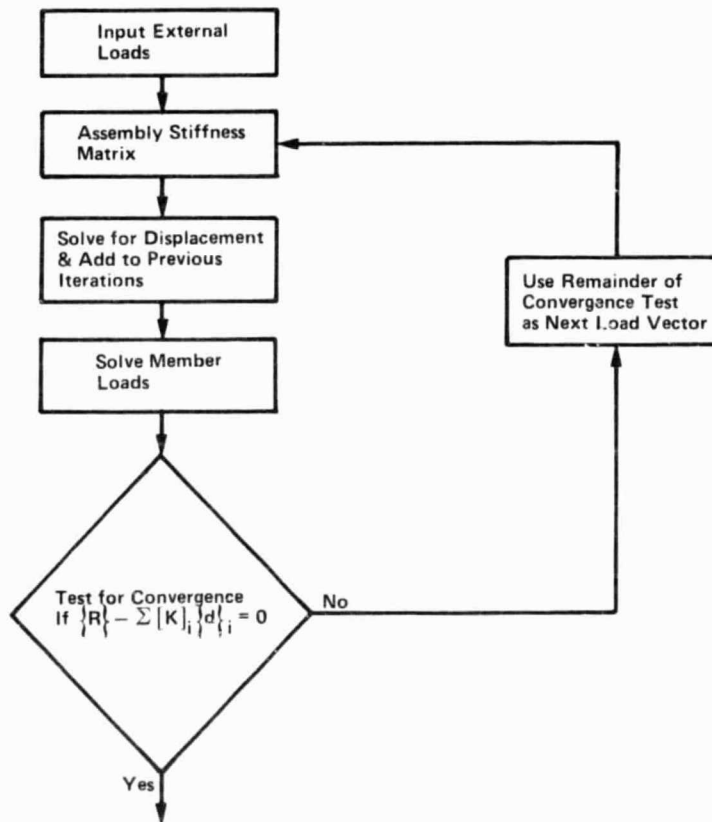


Figure 24 Newton-Raphson Solution

Once the stiffness matrix is assembled, which includes the stress stiffening terms, Equation 21 is solved for $\{ \Delta D \}_{i+1}$ using standard linear equation algorithms. The next step is to add ΔD_{i+1} to $\{ D \}$ and to solve for member loads. These are then added together for each node in global coordinates to determine if nodal equilibrium exists in Equation 22.

$$[22] \quad \{R_o\} - \Sigma[k] \{d_{i+1}\} = \{R_{i+1}\}$$

If $\{R\}_{i+1}$ is within $1 \times 10^{-10} N$, the problem is solved. If $\{R\}_{i+1}$ fails the convergence test, it is used as the load vector in the next iteration for which the stiffness matrix is reformulated, and the whole process is repeated. In the example cases run to date, this process has taken only two iterations to solve.

6.3 PRESSURE LOADING

To provide the user a capability to exert pressure loads, e.g., loads from solar pressure, on the tie system model, the loadcase generator allows the user to input a global pressure vector defining the magnitude and direction of pressure in N per m^2 . Unlike most general purpose finite-element solvers the model solver does not require the user to input the pressure load on each element. Instead, the model solver takes the pressure vector and automatically applies it at each node. To take this pressure and distribute it onto the tie system model requires that each pressure vector component be considered separately along with determining the effective mesh area and area ratios for each vector component.

6.3.1 Z Component of Pressure

For a pressure component in the global Z-direction, the effective mesh area is the projected area of mesh on the global X-Y plane times the percent of blockage of the mesh. Assuming the mesh is 90% open in this orientation, for a typical box section, Figure 25, the equation for the projected area is:

$$[23] \quad A_{effz} = 0.10x(X3-X1)x(Y2-Y1)$$

where

X_n = the global X-coordinate of the nth standoff,

Y_n = the global Y-coordinate of the nth standoff,

0.10 = percent of blockage,

A_{effz} = effective mesh area in the X-Y plane.

The total pressure exerted is:

$$[24] \quad P_{tz} = Z_p x A_{effz}$$

where

Z_p = the global Z-component of pressure, and

P_{tz} = total pressure on the tie system in the global Z-direction.

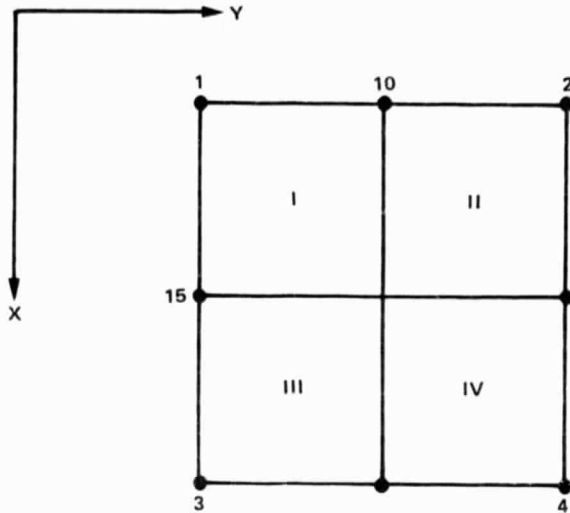


Figure 25 X-Y Plane Projection

To apply this distributed force on the model, the pressure is assumed to be divided equally among all the tie points on the surface and is input onto the model as point loads at the tie point nodes. This assumption that the pressure can be divided equally among the tie points is close to exact because of the fact that the tie points are close to being equally spaced on the surface.

6.3.2 Y Component of Pressure

For a pressure component in the global Y-direction, the effective mesh area is the projected area of the mesh on the global X-Z plane times the percent of blockage of the mesh. Assuming the mesh is only 20% open in this orientation for a typical box section, Figure 26, the equation for the projected area is approximately:

$$[25] \quad A_{effy} = 0.80x((Z_2-Z_{10})x(X_4-X_2)+(Z_{10}-Z_1)x(X_3-X_1))$$

where

X_n = the global X--coordinate of the nth standoff or tie-point,

Z_n = the global Z--coordinate of the nth standoff or tie-point,

0.80 = percent of blockage,

A_{effy} = effective mesh area in the X-Z plane.

The above equation assumes the shaded area in Figure 26 to be the projected area versus the actual area inscribed by the curve in the actual surface. This approximation was assumed for the ease of calculating the area. However, the approximation is very close to the actual projected area.

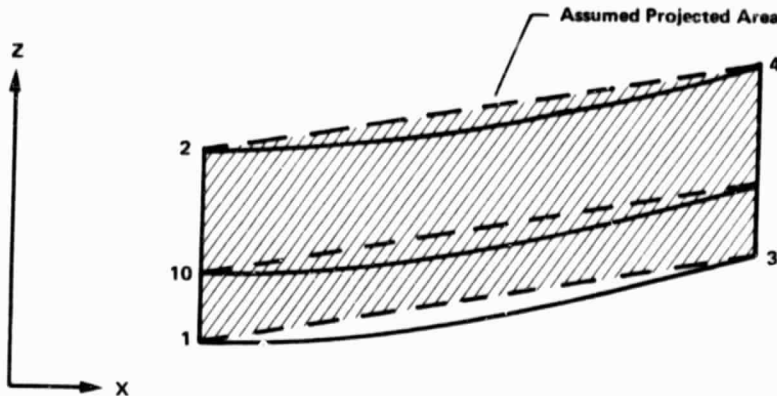


Figure 26 X-Z Plane Projection

The total pressure exerted is:

$$[26] \quad P_{ty} = Y_p \times A_{effy}$$

where

Y_p = the global Y-component of pressure, and
 P_{ty} = total pressure on the tie system in the global Y-direction.

To apply this distributed force on the model, the pressure is divided among the tie points on the surface and is input onto the model as points loads at the tie points. However, unlike the Z component of pressure, the load per tie point is dependent on the projected geometry of the box section, the direction of the pressure vector, and the quadrant location of each tie-point.

For the geometric case when Z_2 is not equal to Z_1 , the point load input on each tie point in quadrants I and III is:

$$[27] \quad F_{py} = (Z_1 - Z_1) / (Z_2 - Z_1) \times P_{ty} / N_{13}$$

where

Z_n = the Z coordinate of the nth standoff or tie-point,
 N_{13} = the number of tie-points in the 1st and 3rd quadrants.

The point load input on each tie-point in quadrants II and IV is:

$$[28] \quad F_{py} = (Z_2 - Z_1) / (Z_2 - Z_1) \times P_{ty} / N_{24}$$

where

Z_n = the Z coordinate of the nth standoff or tie-point,
 N_{24} = the number of tie-points in the 2nd and 4th quadrants.

For the geometric case when $Z_2 = Z_1$ and the pressure vector, Y_p is in the +Y direction; the point input on each tie-point in quadrants I and III is:

$$[29] \quad F_{py} = P_{ty} / (2 \times N_{13})$$

However, the point load input on each tie-point in quadrants II and IV is zero. This is because of the box section geometry is such that the mesh in quadrants II and IV is being shielded by the mesh in quadrants I and III.

For the geometric case when $Z_2 = Z_1$ and the pressure vector, Y_p , is in the -Y direction, the point load input on each tie point in quadrants I and III is zero, and the point load input on each tie point in quadrants II and IV is:

$$[30] \quad F_{py} = P_{ty} / (2 \times N_{24})$$

6.3.3 X-Component of Pressure

For a pressure component in the global X-direction the effective mesh area is the projected area of mesh on the the global Y-Z plane times the percent of blockage of the mesh. Assuming the mesh is only 20% open in this orientation, for a typical box section, Figure 27, the equation for the projected area is approximately:

$$[31] \quad A_{effx} = 0.80 \times ((Z_3 - Z_{15}) \times (Y_4 - Y_3) \times (Z_{15} - Z_1) \times (Y_2 - Y_1))$$

where

Y_n = the global Z-coordinate of the nth standoff or tie point,
 Z_n = the global X-coordinate of the nth standoff or tie point,
 A_{effx} = effective mesh area in Y-Z plane,
 0.80 = percentage of blockage.

As in the Y-component case, this equation is an approximation of the actual area.

The total pressure exerted is:

$$[32] \quad P_{tx} = X_p \times A_{effx}$$

where

X_p = the global X-component of pressure,
 P_{tx} = total pressure on the tie system in the global X-direction.

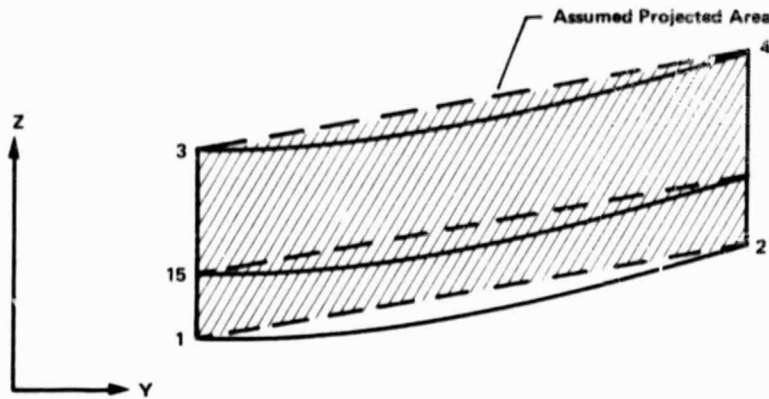


Figure 27 Y-Z Plane Projection

To apply this distributed force on the model, the pressure is divided among the tie points on the surface and is input onto the model as point loads at the tie points. Again, the load per tie point is dependent on the projected geometry of the box section, the direction of the pressure vector, and the quadrant location of each tie point.

For the geometric case when Z_3 is not equal to Z_1 , the tie point load input in quadrants I and II is:

$$[33] \quad F_{px} = (Z_{15} - Z_1) / (Z_3 - Z_1) \times P_{tx} / N_{12}$$

where

Z_n = the Z-coordinate of the nth standoff or tie point,
 N_{12} = the number of tie points in the 1st and 2nd quadrants.

The point load input on each tie in quadrants III and IV is:

$$[34] \quad F_{px} = (Z_3 - Z_{15}) / (Z_3 - Z_1) \times P_{tx} / N_{34}$$

where

Z_n = the Z-coordinate of the nth standoff or tie point,
 N_{34} = the number of tie points in the 3rd and 4th quadrants.

For the geometric case when $Z_3 = Z_1$ and the pressure vector, X_p , is in the +X direction, the point load per tie point in quadrants I and II is:

$$[35] \quad F_{px} = P_{tx} / (2 \times N_{12})$$

and the load per tie point in quadrants III and IV is zero. This is because of a similar geometric condition previously discussed for the Y-component of pressure.

For the geometric case when $Z_3=Z_1$ and the pressure vector, X_p , is in the $-X$ direction, the point load per tie point in quadrants I and II is zero and the load per tie point in quadrants III and IV is:

$$[36] \quad F_{px} = P_{tx} / (2xN34)$$

7.0 SURFACE TOPOGRAPHY SOLVER

The surface topography solver conducts an analysis to determine the systematic and random errors that distort the surface. This is done through two routines, the interpolation routine and the "best-fit" surface routine.

The surface is defined according to the type of interpolation technique chosen by the user. The interpolation routine takes the distortions of the user specified box sections from the model solver and creates distortions for the entire reflector through linear interpolation. As mentioned in Section 2.1, there are three types of interpolation techniques:

- 1) Worst case technique,
- 2) One-dimensional interpolation technique,
- 3) Two-dimensional interpolation technique.

For the worst-case technique, since there is no interpolation performed, i.e., the surface is defined as that section of the reflector within the box section in question. For either the one- or two-dimensional interpolation technique, the surface is defined as the entire reflector. Overviews and uses of these three techniques are given in Section 2.1.

Once these distortions have been determined, the "best-fit" surface routine adds them to the original, undisturbed surface to form the distorted surface. In the case of the choice of worst- case technique, the distortions obtained from the model solver are added to the original surface. Next, mesh manufacturing errors are added to the distorted surface. This is done by using a normal distribution curve and a random number generator to create random translations in the Z-direction. This normal distribution curve uses the user's specified manufacturing error tolerance as the 3σ value. The "best-fit" surface routine then takes the distorted surface and finds a "best-fit" paraboloidal surface, from which systematic and random errors are found. These errors are then converted to parameters that the rf performance program is capable of using.

7.1 INTERPOLATION ROUTINE

The interpolation routine is performed for both one- and two-dimensional interpolation techniques. It interpolates the distortions between any two box sections to find the distortions for the in between box sections.

Translations of each node of the first box section are interpolated independently with the translations of each corresponding node of the second box section, e.g., in the example of Subsection 2.1.2, (Fig. 5), the X-translation of node 10101 of a box section in Line 1 is linearly interpolated with the X-translation of node 10101 of a box section in Line 4. This is done for each of three translations for each node. The need for one-to-one correspondence among nodes is now evident.

7.2 "BEST-FIT" SURFACE ROUTINE

The purpose of this routine is to determine the systematic and random movements of the reflector surface. This is achieved by manipulating a perfect surface to "best-fit" the distorted surface. These manipulations, roll, pitch, change in focal length, and vertical movement, all contribute to systematic error and are illustrated in Figure 28. The difference in the Z-coordinate of node on the distorted surface and the Z-coordinate of its corresponding node on the perfect surface is defined as the random error. The "best-fit" surface is that paraboloidal surface that shows a minimum rms of random surface error, Equation 37.

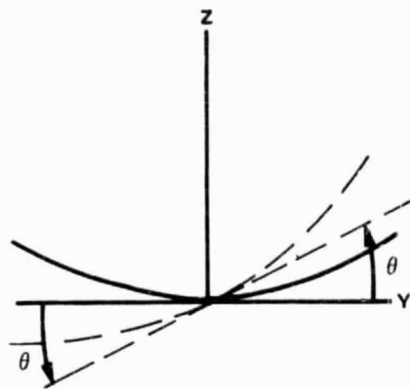
$$[37] \quad \text{rms} = \sqrt{\frac{\sum_{i=1}^N (Z_d - Z_p)^2}{N}}$$

where

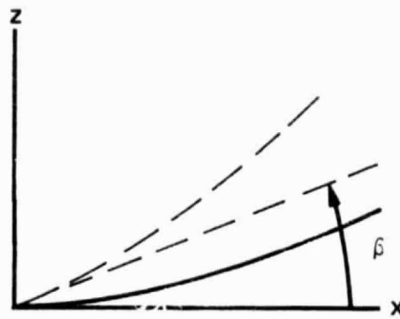
Z_d = Z-coordinate of a node of the distorted surface,
 Z_p = Z-coordinate of a node of the "best-fit" surface,
 N = total number of nodes on the surface,
 rms = rms of random surface errors.

The perfect surface is manipulated through a series of orderly iterations. Initially, the perfect surface is moved vertically, with no change in focal length, pitch, or roll, until a minimum rms is found. At this point, the focal length is incremented and the surface is again moved vertically until a minimum rms is found. This rms is compared to the previously found minimum rms and, if less, is retained as the minimum rms. After the focal length has completed its changes, the pitch is incremented and the focal length and vertical movement are again varied to find the minimum rms. The last movement is the roll of the surface, for which the pitch, focal length, and vertical movement are all varied to find minimum rms. At the end of these iterations, a perfect paraboloidal surface is found, with its corresponding surface definitions of minimum rms, vertical movement, focal length, pitch, and roll.

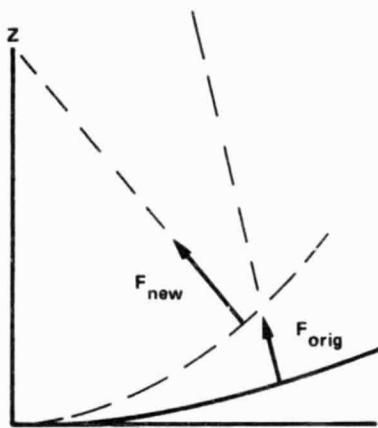
These surface definitions are now converted into usable variables for the rf performance program. The rf performance program incorporates the three systematic movements, roll, pitch, and vertical movement, into equivalent defocusing in the X, Y, and Z directions, Equations 38, 39, and 40.



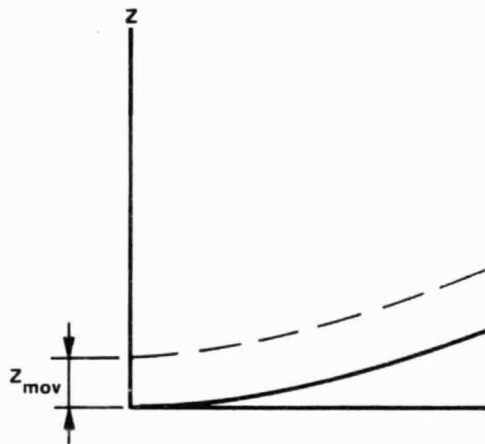
(A) ROLL MOVEMENT



(B) PITCH MOVEMENT



(C) FOCAL LENGTH CHANGE



(D) VERTICAL MOVEMENT

Figure 28 Surface Movements

[38] Defocusing in $X = F \times \theta / 2$

[39] Defocusing in $Y = F \times \beta / 2$

[40] Defocusing in $Z = F - F_{bf} - Z_{mov}$

where

F = focal length of original surface,

F_{bf} = focal length of "best-fit" surface,

β = pitch of the "best-fit" surface,

θ = roll of the "best-fit" surface,

Z_{mov} = vertical movement of the "best-fit" surface.

The rms of surface error found in the "best-fit" routine is added to the rms of surface error because of pillowing to find a total system rms, which is used in the Ruze equation.

The rf performance program conducts analyses for four cuts, at 0, 90, 180, and 270 degrees. Each cut is analyzed from boresight through the first sidelobe, which is assumed to be within $213\lambda/D$ degrees off boresight.

A card image deck for use in the rf performance program is provided as a convenience to the user.

The last program in the Integrated Mesh Analysis System is the rf performance solver. This program calculates the far-field patterns of spherical or parabolic reflector antennas. In addition, the program is capable of determining the beam efficiency of the antenna pattern. The results of the surface topography solver are used to define the antenna geometry, while the model generator defines the other antenna parameters for this program. The antenna geometry and parameters include the operating frequency, aperture size, feedhorn size, feed location, and surface roughness. Additionally, the surface topography solver calculates the grid pattern of points, the number and orientation of pattern cuts, and the limits and increment of each pattern cut to ensure accurate results from the rf performance solver.

The technique of aperture integration, also known as the Aperture Field Method, is used to calculate the far zone patterns. The major portion of the program was written by the Ohio State University ElectroScience Laboratory for Martin Marietta Denver Aerospace. However, added to the program was a subroutine to calculate the beam efficiency of the reflector. This subroutine requires that the far-field pattern of the main beam and first side lobes for four surface cuts be calculated by the main program. The surface cuts represent the E and H planes for the reflector. The method by which the beam efficiency is calculated is discussed later. The algorithms to determine the far-field pattern were adapted from the NEC reflector code. Consequently, only the main beam and near sidelobes (typically 3 to 10 beamwidths) can be accurately computed. This approach is sufficient for determining the beam efficiency of an antenna. The following are excerpts from the OSU Final Technical Report 713581-2, "Computer Code for Spherical and Parabolic Torus Reflector Antennas."

8.1 APERTURE INTEGRATION

This basic method has been applied to compute the radiation patterns of reflector antennas for many years. It states that the radiated field of an aperture antenna can be determined by the field distribution on the aperture. Thus,

$$[41] \quad \bar{E} = \frac{jk}{2\pi} \iint [\bar{F}_x E_x^a + \bar{F}_y E_y^a] \frac{e^{-jks}}{s} dx dy.$$

for a reflector with its axis coincident with the z-axis and with its aperture defined in the x-y plane. E_x^a and E_y^a are the x- and y-components of the aperture field. F_x^a and F_y^a are the modified vector element patterns associated with two Huygen's sources (crossed electric and magnetic dipoles) each having its electric field vector parallel to the x- and y-axis, respectively. These vector element patterns are expressed by

$$[42] \quad \bar{F}_x = [\hat{\theta} \cos\phi - \hat{\phi} \sin\phi] \cos\left(\frac{\theta}{2}\right).$$

and

$$[43] \quad \bar{F}_y = [\hat{\theta} \sin\phi + \hat{\phi} \cos\phi] \cos\left(\frac{\theta}{2}\right).$$

$$\rho = \sqrt{x^2 + y^2}$$

Numerically, the aperture fields are calculated at the grid points and stored. Therefore they can be used for different pattern cuts without being recalculated.

8.2 ROTATING GRID METHOD

The aperture integration method requires a two-dimensional integration for each pattern point as indicated in Equation 42. However, for far-field computations, an appropriate rotation of the grids greatly improves the efficiency in carrying out the integration.

With this approach the y -integration is carried out for each column of the aperture and each one-dimensional integration result is stored. The stored values for the y -integrations are then used for each pattern angle θ in the plane perpendicular to the y -axis, thus, the efficiency approaches that of a one-dimensional integration. By using this technique, the number of sum operations for the far-field integration is $M(M+N)$ where M represents the maximum total number of rotated grid lines and N the number of far-field observation angles. The number of sum operations for the usual two-dimensional integration would be MxN^2 for a square grid. The ratio of the number of operations for the two methods is MxN to $M+N$. As an example, for a 40×40 grid with 80 AI pattern angles, the rotating grid method is 27 times more efficient than the nonrotated grid method.

8.3 GEOMETRY FOR THE REFLECTOR SURFACES

The coordinate system used to describe the reflector surface is defined in this section. Equations for the normal vectors and principal radii of curvature on the surface are given later. These quantities are necessary for the ray tracing procedure and described in the following sections.

In all cases, the aperture plane is perpendicular to the z -axis, and as close to the reflector rim as possible. For example, the perimeter of a round reflector rim will touch the aperture plane everywhere, whereas a square reflector will touch the aperture plane at only four points.

The geometry relevant to either a parabolic or spherical reflector is shown in Figure 29. The surface of revolution is described by the FZ function, where

For a parabola,

$$[44] \quad FZ(\rho) = \frac{\rho^2}{4F} - \begin{cases} ZREF1; & NR=1 \\ 0; & NR=0 \end{cases}$$

For a sphere,

$$[45] \quad FZ(\rho) = 2F - \sqrt{(2F)^2 - \rho^2} - \begin{cases} ZREF1; & NR=1 \\ 0; & NR=0 \end{cases}$$

If $NR=0$, the origin is at the vertex of the surface. Otherwise, it is at the aperture plane $z=ZREF1$ as shown in Figure 29.

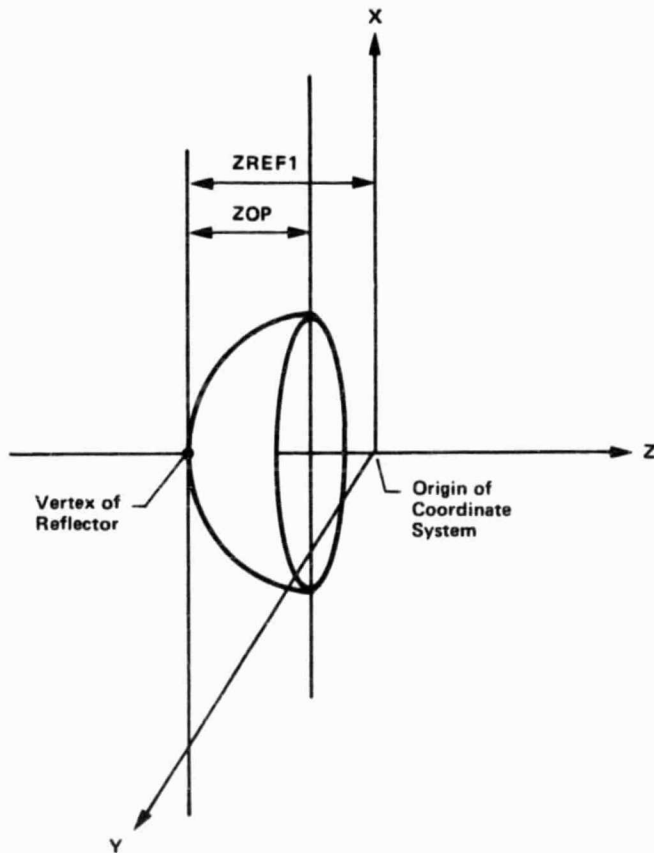


Figure 29 Coordinate System for a Surface Revolution

8.4 CALCULATION OF THE APERTURE FIELDS

To calculate the aperture fields over the principal grid, a ray tracing procedure is used. The relevant quantities are illustrated in Figure 30.

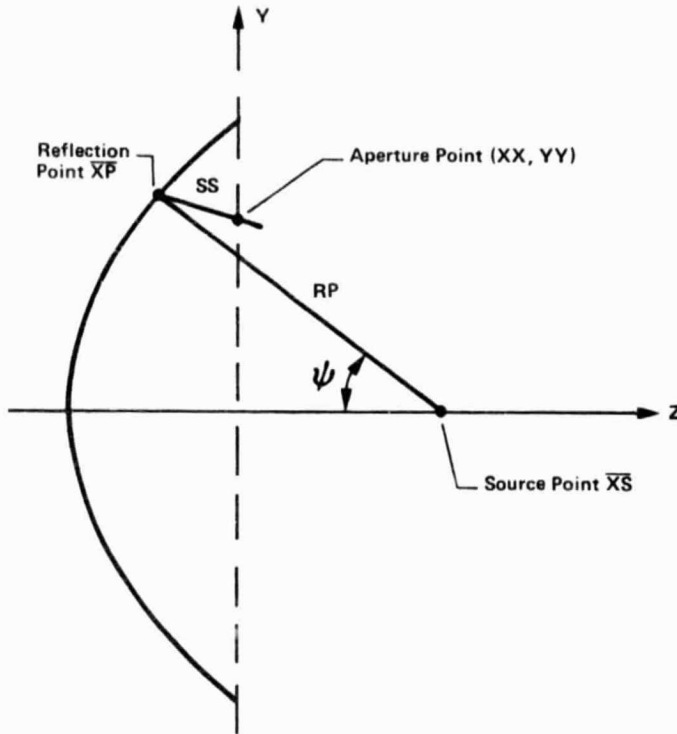


Figure 30 Geometry of Ray Tracing to Aperture Field Point

Once the ray tracing procedure is completed for a specific aperture point, the aperture field can be calculated. To accomplish this, the feed pattern angles to the reflection point \overline{XP} are first calculated as

$$[46] \quad \phi' = \text{PHIPR} = \tan^{-1} \frac{XP(2) - XS(2)}{XP(1) - XS(1)}$$

$$[47] \quad \psi = \text{PSIR} = \tan^{-1} \frac{[(XP(1) - XS(1))^2 + ((XP(2) - XS(2))^2)]^{1/2}}{-(XP(3) - XS(3))}$$

where \overline{XS} is the phase center of the feed. These angles are needed to calculate the rectangular vector components for the \overline{E} field of the feed pattern at the reflection point, \overline{XP} .

The incident feed pattern at XP is given by

$$[48] \quad \overline{E}^i = \hat{x}E_{IX} + \hat{y}E_{IY} + \hat{z}E_{IZ}$$

Reflection from the reflector surface, \overline{E}^r , is calculate by

$$[49] \quad \vec{E}^r = \hat{x}ERX + \hat{y}ERY + \hat{z}ERZ.$$

The aperture field at (XX, YY) is obtained by including pathlength effects in Er as follows:

The aperture field at (XX,YY) is obtained by including pathlength effects in Er as follows:

$$[50] \quad EA_x = F \cdot ERX \cdot \frac{PHSEA}{RP}$$

$$[51] \quad EA_y = F \cdot ERY \cdot \frac{PHSEA}{RP}$$

where

F = focal distance of the reflector
-jk (ROS)

PHSEA = e,
and ROS = RP + SS.

8.4.1 Ray Tracing

The rf performance program calculates the reflection point XP from an estimate, XPO, that is based on a focussed parabola. The geometry is shown in Figure 31. We have

$$\begin{aligned} XPO(1) &= XX, \\ XPO(2) &= YY, \\ XPO(3) &= FZ(XP(1),XP(2)). \end{aligned}$$

The closer XPO is to XP, the better. However, an iterative procedure will converge quickly even if XPO is a poor estimate of XP, i.e., ten wavelengths off.

A "local" coordinate system is set up as shown in Figure 32. Its origin is at the estimate XPO, and its axes are along the principal directions of the surface. The surface is approximated as quadratic in the neighborhood of XPO. Thus, the equation of the local surface becomes

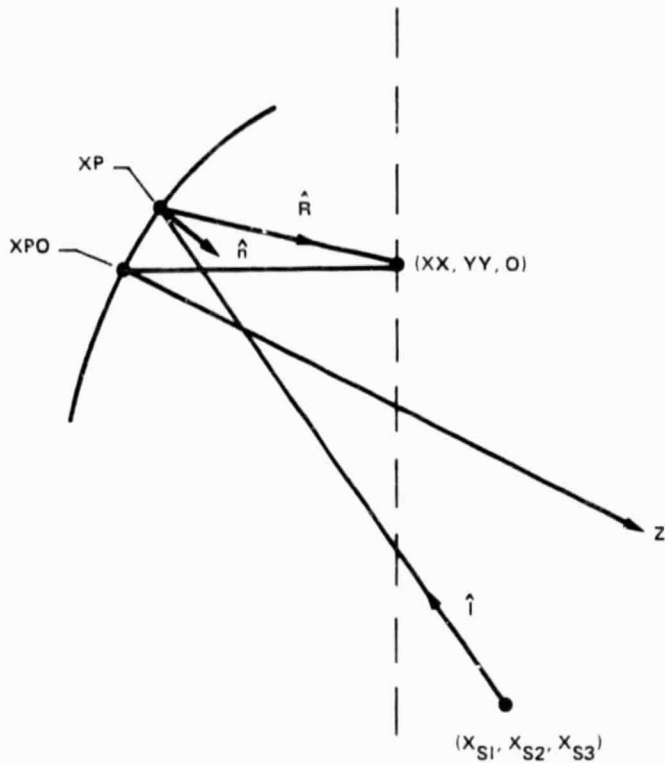


Figure 31 Reflection Point XP , and its Estimate XPO

$$[52] \quad z = f(x,y) = \frac{1}{2} \left(\frac{x^2}{R_x} + \frac{y^2}{R_y} \right)$$

where R_x and R_y are the principal radii of curvature of the surface at the reference point XPO .

The normal at the reflection point XP in Figure 28 may then be approximated by

$$[53] \quad \bar{n} = - \frac{\partial f}{\partial x} \hat{x} - \frac{\partial f}{\partial y} \hat{y} + \hat{z}$$

so that

$$[54] \quad \bar{n} = - \frac{x}{R_x} \hat{x} - \frac{y}{R_y} \hat{y} + \hat{z} .$$

This approximation is valid if the reflection point XP is sufficiently close to the reference point XPO such that Equation 54 is valid, and provided x and y are small compared to z . The incident and reflected vectors as shown in Figure 32 are given by

$$[55] \quad \bar{I} = (x - x_o) \hat{x} + (y - y_o) \hat{y} + (z - z_o) \hat{z} .$$

$$[56] \quad \bar{R} = (x_t - x) \hat{x} + (y_t - y) \hat{y} + (z_t - z) \hat{z}$$

The law of reflection at XP requires

$$[57] \quad (\bar{n} \cdot \bar{I})(\bar{n} \times \bar{R}) + (\bar{n} \cdot \bar{R})(\bar{n} \times \bar{I}) = 0 .$$

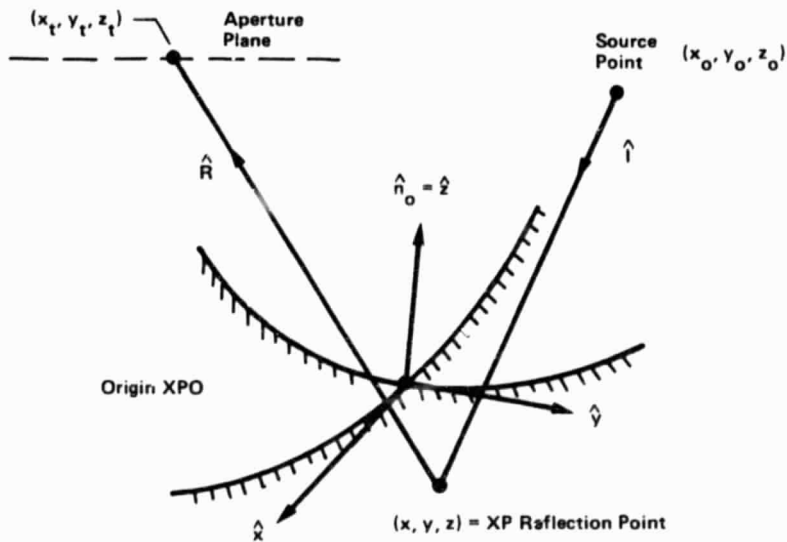


Figure 32 Local Coordinates at XPO on Doubly Curved Surface

Substituting Equations 54, 55, and 56 into Equation 57 yields three nonlinear simultaneous Equations in three unknowns $x, y,$ and z . Since x and y are small, we may drop the higher order terms, leaving three linear equations in three unknowns.

The resulting equations are given by

$$[58] \quad - \left(\frac{x_o y_t + x_t y_o}{R_x} \right) x - \left(\frac{2(y_o y_t - z_o z_t)}{R_y} + z_o + z_t \right) y$$

$$[59] \quad \left(\frac{2(x_o x_t - z_o z_t)}{R_x} + z_o + z_t \right) x + \left(\frac{x_t y_o + x_o y_t}{R_y} \right) y$$

$$[60] \quad \left(\frac{y_o z_t + y_t z_o}{R_x} \right) x - \left(\frac{x_o z_t + x_t z_o}{R_y} \right) y = 0 .$$

Because of the approximation, the rf performance program verifies the accuracy of the ray tracing. If the aperture plane point (XX,YY) is in error by more than 0.1 the calculation of XP is repeated. By looping through all the horizontal and vertical grid lines, a two dimensional array of the aperture fields is calculated.

8.5 BEAM EFFICIENCY

Beam efficiency is the ratio of the pattern power within the main beam to the total pattern power. To calculate the beam efficiency of the antenna system requires that the aperture field pattern of the E and H planes be determined. The subroutine that determines beam efficiency takes the aperture field pattern and determines the beam width first null, i.e., the angle off boresight that defines the main beam for each plane. Then the power in the main beam for each plane is determined by integrating the main beam pattern over the boresight angle using Simpson's rule. Finally, the total power in the main beam for each plane is summed and the average found. This average total power in the main beam is then divided by four. The result is the beam efficiency of the reflector excluding effects because of surface roughness. The following describes the methodology that allows the beam efficiency to be calculated in this manner.

Since beam efficiency is defined as the ratio of the power in the main beam to the total pattern power the following is true in terms of radiation intensity, U

where U includes both polarizations is necessary. Assuming that the pattern is close to uniform for any pattern cut, and for paraboloidal reflectors, the denominator is equal to:

$$[61] \quad \text{Beam Efficiency} = \frac{\int_{-\theta}^{\theta} \int_0^{\pi} U(\theta, \phi) \sin\theta \, d\phi \, d\theta}{\int_{\pi}^{\pi} \int_0^{\pi} U(\theta, \phi) \sin\theta \, d\phi \, d\theta}$$

This reduces Equation 61 to

$$[62] \quad \text{Beam Efficiency} = \frac{\pi \times \text{Directivity} \int_{-\theta}^{\theta} U(\theta) \sin\theta \, d\theta}{4\pi U_{\max}}$$

Finally, since the directivity is equal to U_{\max} , the equation further reduces to

$$[63] \quad \text{Beam Efficiency} = \frac{\int_{-\theta}^{\theta} U(\theta) \sin\theta \, d\theta}{4}$$

Since the pattern cuts from the program exclude surface roughness effects, this ideal beam efficiency is adjusted by using the following form of the Ruze equation. The rms surface error that is used was determined by the Surface Topography Solver.

$$[64] \quad \text{Beam Efficiency} = \text{Beam Efficiency(ideal)} * \exp(-4 X_{\text{rms}}/)^{**2}$$

Using the Integrated Mesh Analysis System, a study was performed to determine the performance improvements possible when using active mesh surface control. The baseline box truss mesh antenna used in this study was the Earth Observation Spacecraft (EOS), as defined in NASA CR-3689 (Fig. 33).

The EOS is a complete earth orbiting remote sensing platform that uses a large microwave radiometer as the "core" instrument. Radiometer antennas are especially sensitive to mesh performance since the beam efficiency is extremely critical to radiated energy collection. With active mesh surface distortions can be minimized and, therefore, result in performance improvements.

Active mesh control was achieved by incorporating linear actuators at the bottom of the standoffs. This allows the surface to be adjusted in the opposite direction of the surface distortions caused by operating conditions. This is the simplest and most cost-effective method for adding active mesh control to the EOS structure, i.e., a single-linear actuator at the root of each standoff (Fig. 34). This system of on-orbit correction is limited to control motions along the reflector's Z-axis only. However, moving the standoffs along the Z-axis usually provides enough surface adjustment to significantly improve the performance characteristics of the reflector. Also, having a linear actuator at each standoff allows each standoff to be moved independently thus providing the best possible surface improvement.

ORIGINAL PAGE IS
OF POOR QUALITY

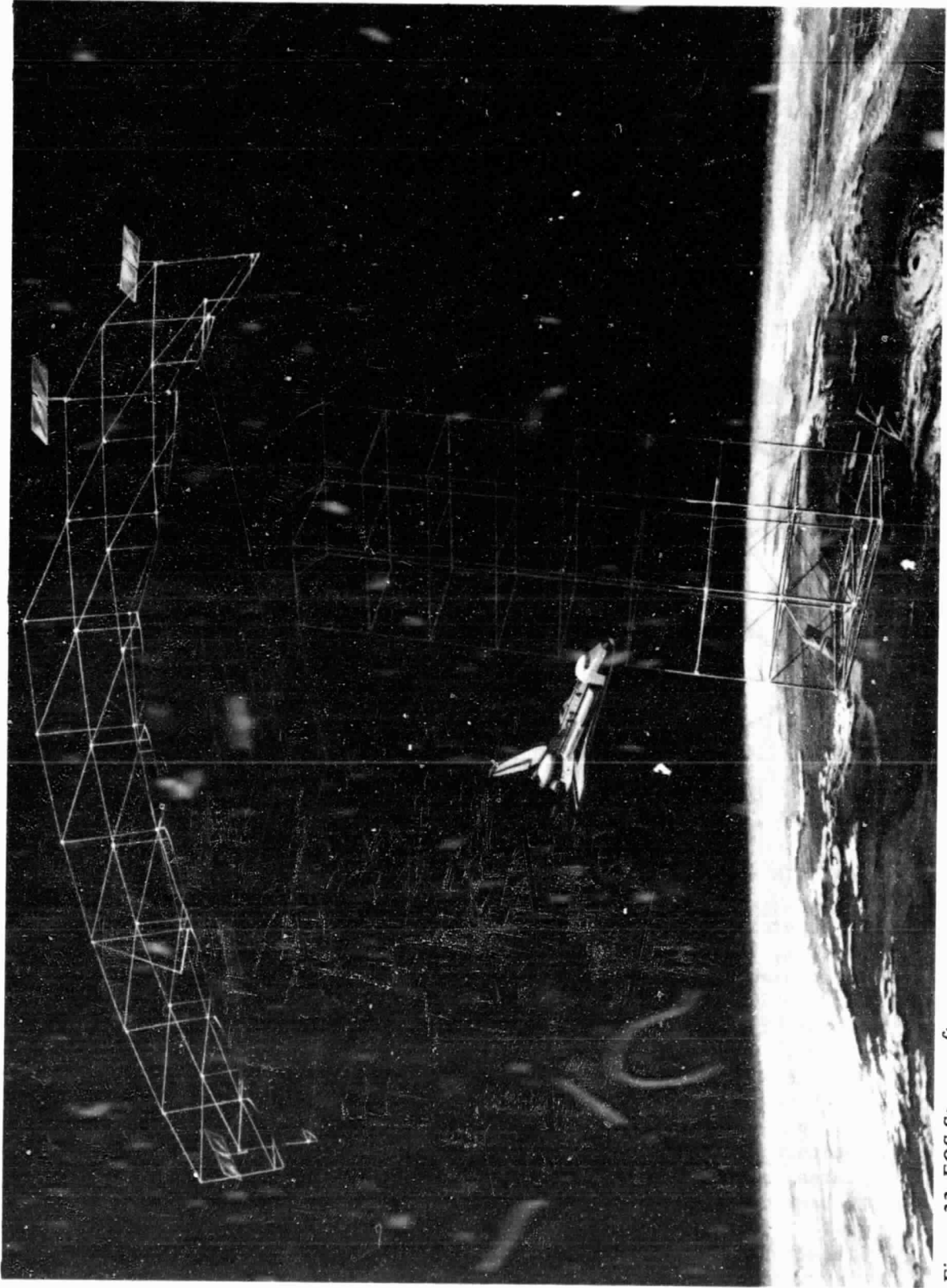


Figure 33 EOS Spacecraft

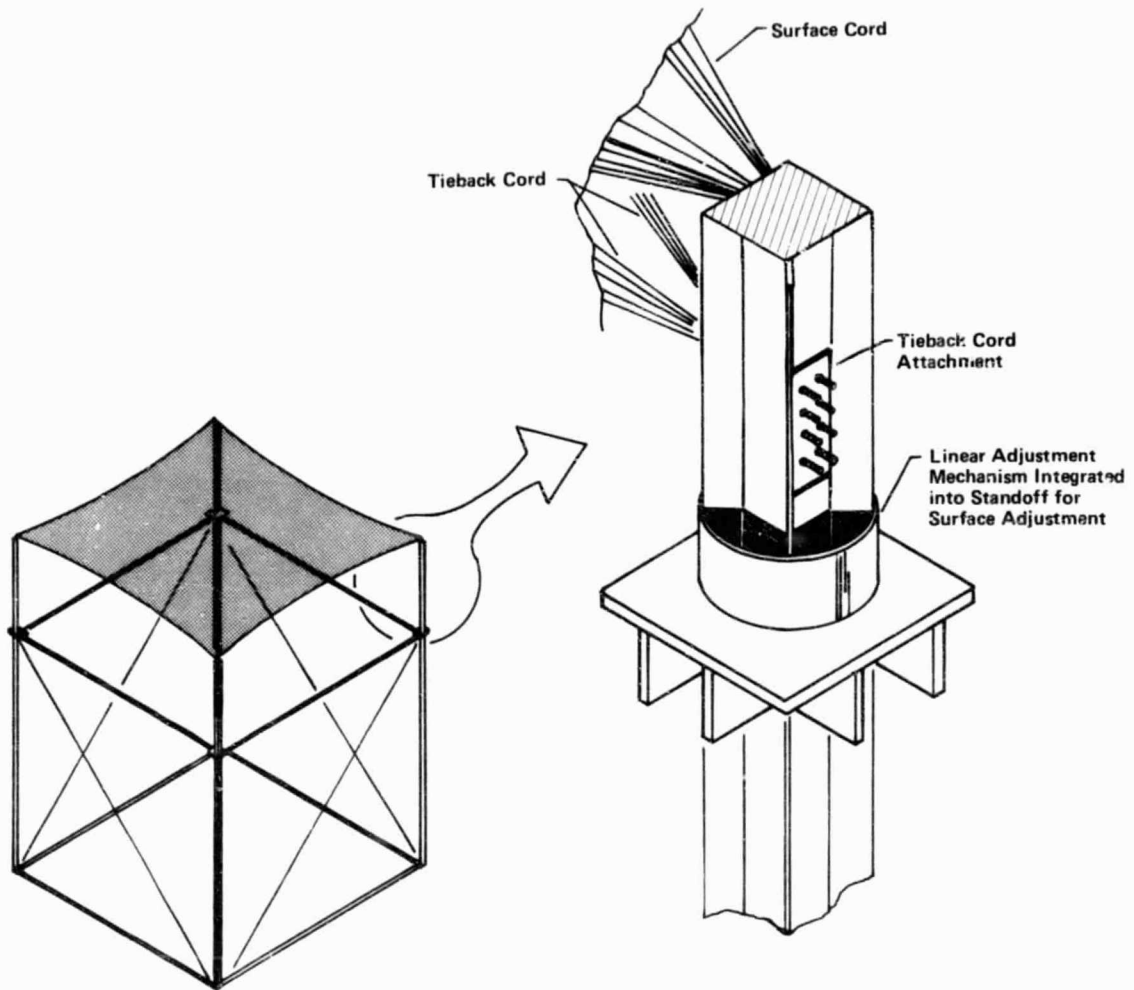


Figure 34 Typical Linear Actuator System

9.1 ANALYSIS METHOD

To determine the performance improvements because of active surface control, the EOS reflective surface was modeled and analyzed using the Integrated Mesh Analysis System. Since actual operating environments for the EOS were not severe enough to impose loads or cause distortions worthy of onorbit correction, two fictitious thermal environments were chosen. Generally, thermal environments that cause a large differential between the surface cord temperatures and tieback cord temperatures cause the largest amount of surface distortion. Therefore, the thermal environments used in this study applied a relatively large temperature differential to the EOS reflective surface by imposing temperatures on only the tieback cords. The first thermal case heated the tieback cords while the second case cooled the tieback cords.

Since box truss distortions were not analyzed for such an environment, they were not included in this analysis. Also, the truss manufacturing errors were not included in this study since it is assumed that they

will be compensated for in the original installation of the standoffs. However, manufacturing errors for the tie system and mesh pillowing were included. The manufacturing tolerance for tying the mesh surface was assumed to be +0.0625 cm. The mesh pillowing resulted from using a tie spacing of 0.7 meters--the tie spacing value used in the previous EOS study.

9.2 EOS TIE SYSTEM DESIGN

The EOS tie system design, generated by the model generator, consisted of the center feed and a surface of 4x4 box sections representing the center 60-meter reflector spot of the complete EOS surface, as shown in Figure 35. A one-dimensional interpolation technique was employed to determine the surface distortions. This required two box sections of mesh to be modeled and analyzed in detail. Therefore, two opposite edge box sections were used, i.e., box 102 and 402 (Fig. 35). Using a tie spacing of 0.7 meters resulted in 1222 tie points per 15 meter box section. To reduce the cost of analysis and to fit the analytical model into the available computer memory, the analytical model was reduced to 80 tie points per box section, (i.e., a 6.5% analytical model). The resulting number of finite elements representing the tie cords was 206 with 110 representing the surface cord segments and 96 representing the tieback cords.

The surface and tieback cords both used graphite for the material, with a cross-sectional area of 2.32×10^{-7} and 1.16×10^{-7} m², respectively. This is different from the previous EOS study, which used larger cords for the tiebacks than for the surface cords. During the course of verifying the Integrated Mesh Analysis System, it was determined that larger surface cords make for a more stable tie system. Therefore, this design change was incorporated into this study. The standoffs used in the analytical model were the same cross-sectional size and design as the previous EOS study. However, because of design improvements incorporated into the mesh tie system model generator, the standoffs were reduced in length from 2.0 to 0.5 meters. Figure 36 shows the cross section and material properties for a typical standoff. The other input parameters used in the tie system model generator that defined the overall reflector (i.e., feed type, edge taper, and frequency of operation) are shown in Table 7.

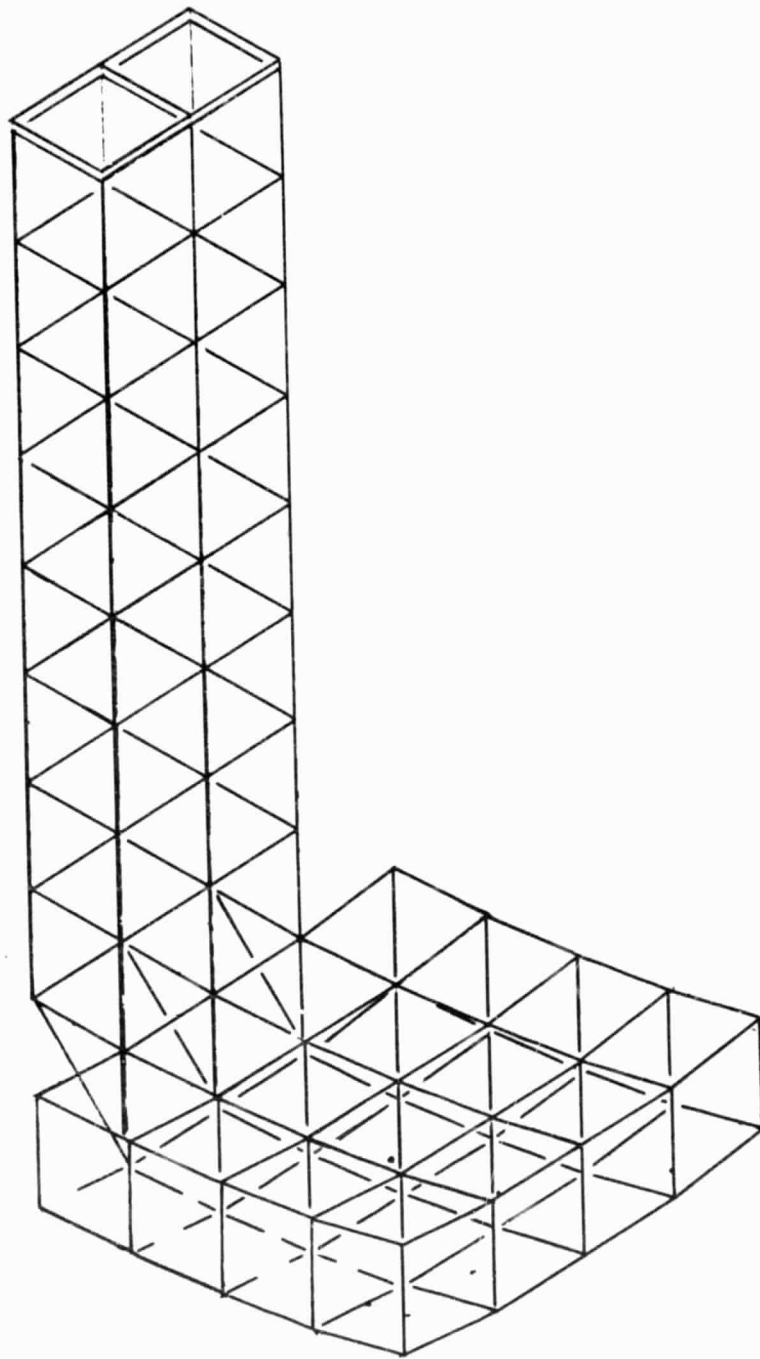
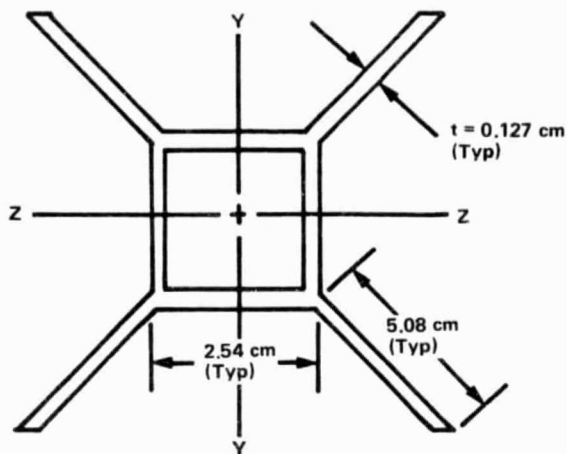


Figure 35 60-Meter Section of EOS



$$\begin{aligned} \text{Area} &= 3.81 \text{ cm}^2 \\ I_{YY} = I_{ZZ} &= 27.53 \text{ cm}^4 \\ J &= 55.06 \text{ cm}^4 \end{aligned}$$

Member 2

Layup (45F/OT₃/45F₂/OT₃/45F) T = Tape
F = Fabric

Material Used

- Tape - Pitch 75
- Fabric - T300

$$E_L = 1.82 \times 10^{11} \text{ N/m}^2 = \text{Longitudinal Modulus}$$

$$E_T = 0.219 \times 10^{11} \text{ N/m}^2 = \text{Transverse Modulus}$$

$$G_{LT} = 0.143 \times 10^{11} \text{ N/m}^2 = \text{Shear Modulus}$$

$$\nu_{LT} = 0.35 = \text{Poisson's Ratio}$$

$$CTE_L = -0.522 \times 10^{-6} \text{ m/m/C} = \text{Coefficient of Thermal Expansion in Longitudinal Direction}$$

Figure 36 Standoff Member

Table 7 Tie System Model Generator Inputs

Feed Type = Corrugated Horn
Edge Tape of Feed = 14.3 dB
Frequency of Operation = 5.5 GHz

9.3 ANALYSIS CASES

For each thermal environment, two separate analysis cases were performed. The first two cases determined the system errors on the antenna without any active mesh surface adjustment--Loadcases 1 and 2. The second two cases determined the system errors after active surface adjustment--Loadcases 3 and 4. The amount of surface adjustment for Loadcases 3 and 4 were determined by averaging the distortions from Loadcases 1 and 2 per quadrant and per box. Table 8 defines the thermal environments that were applied to the mesh tie system model to represent a relatively large differential between the surface cords and the tieback cords. As an example, the 200 C applied to the tieback cords in box 102 for Loadcases 1 and 3 represent an effective temperature differential of 178 degrees between the surface cords and tieback cords.

Table 8 Temperature Values on Mesb Tie Cords

Thermal Loadcase	Surface Cord Temp, °C		Tieback Cord Temp, °C	
	Box 102	Box 402	Box 102	Box 402
1 & 3	22.0	22.0	200.0	300.0
2 & 4	22.0	22.0	-100.0	-150.0
Reference Temperature = 22.0 Degrees				

The temperatures applied to the standoffs were unchanged from the actual maximum and minimum solar flux cases found in the EOS report. Table 9 defines the temperatures applied to the standoffs.

Table 9 Temperature Values on Standoffs

Thermal Loadcase	Box 102 Standoffs, °C				Box 402 Standoffs, °C			
	1	2	3	4	1	2	3	4
1 & 3	-42.5	-46.9	-48.6	-44.0	-42.0	-44.7	-48.6	-47.4
2 & 4	-106.2	-106.2	-106.6	-106.0	-105.1	-105.0	-100.4	-100.1

To apply the surface adjustment to the bottom of each standoff, specified displacements along the Z-axis were input into Loadcases 3 and 4 at node points 6, 7, 8, and 9. Recall from Section 4.2 that the bottom of the standoffs are represented in the analytical model by nodes 6,7,8, and 9. The required surface adjustment per box section is shown in Table 10.

Table 10 Standoff Movement to Adjust for Surface Distortions

Thermal Case	Box	Node	Standoff	Standoff Movement along the Z-Axis, m
3	102	6	1	1.729E-3
		7	2	1.744E-3
		8	3	1.715E-3
		9	4	1.729E-3
	402	6	1	2.883E-3
		7	2	2.920E-3
		8	3	2.772E-3
		9	4	2.775E-3
4	102	6	1	-1.618E-3
		7	2	-1.620E-3
		8	3	-1.620E-3
		9	4	-1.618E-3
	402	6	1	-1.687E-3
		7	2	-1.711E-3
		8	3	-1.707E-3
		9	4	-1.686E-3

9.4 ANALYSIS RESULTS

Table 11 summarizes the results from the model solver, surface topography solver, and rf performance solver for each of the four loadcases.

By comparing the surface adjusted in Loadcases 3 and 4 with the unadjusted Loadcases 1 and 2, it can be seen that the linear actuator system used to adjust the surface shape was effective in reducing the global surface movements, i.e., the equivalent feed movement of the

reflector. However, the linear actuator system was ineffective in changing the surface roughness, i.e, the rms surface error. This because of the fact that the linear actuator system can only move an entire box section surface up or down and has little effect on the tension level within the tie cords. To reduce the surface roughness would require an actuation system that could adjust the cord tension. As an example, in Loadcase 1, the tieback cords were heated thereby reducing their length because of the negative CTE of graphite. This produced higher tensions in all the tie cords and thus moved the tie points within the box section down. This resulted in a negative global Z movement of the surface equal to 4.418 cm and also produced a relatively large rms surface error of 0.2080 cm. Loadcase 3 adjusted the bottom of each standoff up, and thus, reduced the global Z movement to 0.45 cm. However, the rms surface error stayed virtually unchanged at 0.1996 cm. This global correction caused the beam efficiency to increase from 74.0 to 75.3%. Since Loadcase 2, i.e, cooling the tieback cords, did not produce the large global antenna movements and instead caused larger rms surface errors, the linear actuator system had little effect on improving the antenna performance. Because the reflector used in this study had an $F/D = 2.0$, the reflector can withstand substantial global distortions before causing significant antenna degradation.

Although the improvements shown in this study may not seem significant, previous studies on reflector systems with F/D ratios of approximately 0.5 have shown that the global distortions of the box truss support structure, reflector tie system, and feed beam can cause significant degradation in antenna performance. With the linear actuator system, these distortions could be reduced significantly and therefore improve the antenna performance. If the requirement exists that the surface roughness must be reduced, then a second surface adjustment system must be incorporated into the design. Possibly an adjustment system that allows the movement of groups of tieback cords.

Table 11 Results of Onorbit Surface Adjustment

Thermal Loadcase	Maximum Tie Point Distortion, cm	Equivalent Feed Movement, cm X-Axis Y-Axis Z-Axis	RMS Surface Error, cm	Halfpower Beamwidth, deg	Antenna Gain, dB	Beam Efficiency
1	-1.60 (in Box 402)	0.405 0.202 -4.418	0.1869 w/o Pillowing 0.0211 Pillowing 0.2080 Worst-Case Sum	0.08	67.50	74%
2	1.178 (in Box 402)	0.0 0.0 -0.452	0.2450 w/o Pillowing 0.0211 Pillowing 0.2661 Worst-Case Sum	0.08	66.83	64%
3 (Adjusted Loadcase 1)	-0.53 (in Box 402)	0.0 0.101 -0.45	0.1785 w/o Pillowing 0.0211 Pillowing 0.1996 Worst-Case Sum	0.07	67.53	75.3%
4 (Adjusted Loadcase 2)	1.00 (in Box 402)	0.0 0.0 -0.186	0.2443 w/o Pillowing 0.0211 Pillowing 0.2654 Worst-Case Sum	0.07	66.84	64.1%

The Integrated Mesh Analysis System has been written to provide the user with an analytical tool for predicting box truss mesh antenna performance. The programs let the user choose the level of rigor of analysis. By providing a method for reducing the size of the analytical model and various forms of surface interpolation, a minimum number of reduced box section models can be used to predict antenna performance. This allows the user to perform parametric or preliminary studies on various designs without incurring the usual cost of a rigorous analysis. On the other hand, the user has the option of analyzing the complete surface and the full tie system design to produce an exact analytical model of the reflector surface.

The mesh model generator allows numerous tie system designs to be made within a short period of time. Therefore, the user can change a design quickly and efficiently and predict the impact on the antenna performance because of the design change.

The resulting antenna performance, when using the analysis system includes effects because of manufacturing errors, mesh pillowing, and operating environment loads. The tie system manufacturing errors are added randomly to the mesh tie points using the user's specified manufacturing tolerance. Box truss manufacturing errors can be included in the analysis by specifying displacements at the bottom of the stand-offs. Mesh pillowing is automatically included in the performance analysis by using the user's specified tie spacing and an empirical relationship between tie spacing and pillowing that was developed under the IR&D work at Martin Marietta Denver Aerospace. Operating environment loads are specified by creating Loadcases within the Loadcase generator. These Loadcases can be used to define: (1) point loads at tie points or standoff locations; (2) specified displacements at tie point or standoff locations resulting from truss manufacturing errors or thermal distortions of the box truss; (3) global pressures and/or accelerations resulting from solar pressures or gravity loads; and (4) tie cord temperature changes.

To determine the errors that exist on the reflector surface for a particular tie system design and set of operating conditions, the Integrated Mesh Analysis System solves for a "best-fit" surface by iterating to find the minimum rms surface roughness. This provides a method for separating the systematic or global errors of the antenna reflector from the random errors. The random errors are defined by the rms surface roughness, while the systematic errors are defined by the overall pitch, roll, and vertical displacement of the surface. The system errors are output by the surface topography solver as equivalent feed movements, i.e., feed scanning and axial defocus. The rms surface roughness is used within the Ruze equation to predict rf losses.

By including the random and systematic errors with the aperture integration of the "best-fit" reflector surface, the rf performance solver determines the far-field pattern, including the beam efficiency, and thus the antenna performance of the mesh reflector antenna.

The Integrated Mesh Analysis System is unique since it combines the ability to design, analyze, and predict antenna performance by integrating together the various disciplines of design, finite-element analysis , surface "best-fit" analysis, and rf analysis.

Appendix A
User's Manual

APPENDIX A - USER'S MANUAL

The following is a manual designed to assist in running the Integrated Mesh Analysis System software. The following software was designed for NASA Langley Research Center per contract NAS1-17551, Box Truss Analysis and Technology Development, Mesh Analysis and Control, Task 1.

The software consists of eight separate programs. The first two programs are to be run interactively. The remaining programs are to be run as a batch process job. The job control listing, JCL, for running these programs is shown on page A25.

The user's manual has been divided into separate sections for each program. The procedure to allow communication among these programs is given in this manual. Interactive program prompts and required system commands to be input by the user are shown in **BOLD FACE** print.

A.1 MESH TIE SYSTEM MODEL GENERATOR

NOTE: THIS PROGRAM IS DESIGNED TO BE RUN INTERACTIVELY.

Program filenames:

MESH = Source Program
MESHT = Program Listing
MESHB = Binary Program

Local files required before running program:

NONE

Local files created by the Model Generator:

TAPE13 AND TAPE14 = Top of Standoff Plot Output (OPTIONAL)
TAPE30 AND TAPE31 = Tie Point Plot Output (OPTIONAL)
TAPE15 = Tie System Design Output
TAPE16 = Finite Element Model Output **
TAPE17 = Coordinates of the Surface Node Points
(BINARY) **
TAPE18 = Finite Element Material and Sectional
Properties **

** - indicates files required to be saved for later use

TO RUN PROGRAM

Enter the following system commands after logging onto the system:

GET, MESHB.
MAP, OFF.
MESHB.

ENDING PROGRAM

Enter the following system commands before logging off the system or continuing to run other programs:

REPLACE, TAPE16=pf16. where "pf1" equals a user defined
REPLACE, TAPE17=pf17. permanent filename of five
REPLACE, TAPE18=pf18. characters.
REPLACE, TAPE15=pf15.
REPLACE, TAPE13=pf13, TAPE14=pf14. Use only if plotting option
REPLACE, TAPE30=pf30, TAPE31=pf31. was chosen.

PROGRAM PROMPTS

The following statements in **BOLD FACE** print are the computer generated prompts which will appear while running the program:

1) **ENTER REFLECTOR DIAMETER IN METERS**
?

2> SURFACE TYPES PARABOLIC-(0), SPHERICAL-(1)
FEED TYPES: CENTER FED-(0), OFFSET FED-(1)
ENTER SURFACE TYPE, FEED TYPE

?

2A> ENTER FOCAL LENGTH IN METERS

?

For a spherical surface, respond to 2B>.

2B> ENTER SPHERICAL RADIUS. IF UNKNOWN, ENTER 0. PROGRAM
ASSUMES $R=2F$.

?

3> ARE THE BOXES IDENTICAL (Y OR N)?

?

Input Y when all box sections are of identical size.
If this condition is not met, input N. The program
will skip prompts 4, 4A, and 4B and proceed directly to
the User Generation Section, page A7.

4> BOX TYPES: SQUARE - (0), RECTANGLE - (1)
ENTER BOX TYPE

?

This defines the general shape of the box sections.
For rectangular box sections, respond to 4A>. For
square box sections, respond to 4B>.

4A> ENTER NUMBER OF BOXES IN X-DIR, Y-DIR

?

4B> ENTER NUMBER OF BOXES IN ONE DIRECTION

?

The use of square box sections suggests that the
reflector has the same number of box sections in both
the X and Y directions.

5> WHAT IS THE MANUFACTURING TOLERANCE ON THE TIE SYSTEM IN
METERS

?

Input the maximum manufacturing error allowed.

6> FEED TYPES:REGULAR HORNS-(1), CORRUGATED HORN-(2)
ENTER FEED TYPE

?

6A> WHAT IS THE FEED'S DB EDGE TAPER

?

7) WHAT IS THE FREQUENCY OF OPERATION IN GHZ
?

At this point, the program will output the generated box section numbers with their respective tops of standoffs; the tops of standoffs with their respective coordinate points; and the corner cube points with their respective coordinates.

8) DO YOU WANT A PLOT (Y OR N)?
?

If a plot of the locations of the tops of the standoffs is desired, a grid plot file is created as TAPE13 and TAPE14. TAPE13 contains grid point coordinates, TAPE14 contains the connectivity table.

System will now respond with the following:

CALCULATED OPTIMUM STANDOFF HEIGHT IS xxxxx METERS
WOULD YOU LIKE TO CHANGE THE STANDOFF HEIGHT (Y/N)?

NOTE: INCREASING THE STANDOFF HEIGHT WILL PROVIDE A MORE STABLE TIE SYSTEM, HOWEVER PACKAGING VOLUME WILL INCREASE. DECREASING THE STANDOFF HEIGHT WILL REDUCE THE TIE SYSTEM STABILITY BUT PROVIDE BETTER PACKAGING.

TO ASSURE A STABLE SYSTEM THE MINIMUM STANDOFF HEIGHT ALLOWED IS xxxx METERS.
?

At this point you may respond that you would like to change the standoff height. The system will then respond with:

ENTER NEW STANDOFF HEIGHT IN METERS
?

When the User Generation Section has been used, i.e., all individual box sections are not of identical dimensions, Prompts 9-10 will not appear.

9) INTERPOLATION TECHNIQUES: WORST CASE-(0), 1-D LINEAR-(1),
2-D LINEAR-(2)
ENTER INTERPOLATION TYPE:
?

For worst case technique, respond to 9A).
For 1-D linear technique, respond to 9B) and 9C).
For 2-D linear technique, respond to 9B).

9A) WHICH BOX WILL YOU ANALYZE?

9B) WHICH BOXES WILL YOU INTERPOLATE BETWEEN?

For 1-D linear technique, the following statement will appear:

PLEASE INPUT 2 BOX NUMBERS

For 2-D linear technique, the following statement will appear:

PLEASE INPUT 4 BOX NUMBERS

The first two box section numbers input must be in line with one another in either the X or Y direction. If this condition is violated, the following statement will appear:

**YOUR CURRENT FORMAT WILL NOT ALLOW 2-D INTERPOLATION.
THE FIRST TWO BOXES INPUT MUST BE IN LINE.**

9C> WHICH DIRECTION WILL YOU INTERPOLATE(X OR Y)?
?

This is asked for 1-D linear technique only. Input the direction in which the loading condition varies.

10> HOW MANY SHADOWED BOXES ARE THERE?

Prompts 10> and 10A> will not appear for worst case technique.

10A> ENTER BOX NUMBERS ONE AT A TIME
?

11> ENTER THE NOMINAL TIE SPACING IN METERS
?

For each box section specified for analysis, prompts 12> and 13> will appear. Prompt 14> will appear only once.

**12> DO YOU WANT THE TIE SYSTEM DESIGN PRINTED TO THE SCREEN
(Y OR N)?**

This prompt will allow you to skip the screen output of the tie system design. For tie sytem designs containing large number of tie points this will speed up the running of the program. A hard copy of the tie system design can be output after the run is complete by routing TAPE15 to a printer.

13) DO YOU WANT A PLOT OF THE TIE SYSTEM(Y OR N)?

If a plot of the tie system is desired, input Y and a plotfile will be created as TAPE30 and TAPE31. TAPE30 contains the tie point coordinates. TAPE31 contains the tie cord connectivity.

Before prompt 14), the following message will appear:

ANALYSIS CAN BE PERFORMED ON NO MORE THAN (max. perct.) % AND NO LESS THAN (min. perct.) % OF THE MODEL

This gives the user boundaries for the answer to 14).

14) WHAT % OF THE FULL MODEL WILL BE ANALYZED BY THE FINITE ELEMENT ANALYSIS(%)?

Input this number as a percentage. If the percentage input is outside the boundaries set by the program, the program will not accept the answer and will again prompt 14).

At this point, the user is asked for sectional and material properties.

TIE CORD MATERIAL AND SECTIONAL PROPERTIES

	DEFAULT PROPERTIES	
	GRAPHITE	QUARTZ
MODULUS(PASCALS)	2.34 E11	6.89 E10
DENSITY(KG/CU. M)	1770	2200
CTE(M/M/DEG C)	-0.40 E-6	0.54 E-6

15) SURFACE CORD MATERIAL?

(1)-GRAPHITE, (2)-QUARTZ, (3)-OTHER

?

Prompts 15A), 15D), and 15E) will appear only if the material desired is other than graphite or quartz.

15A) ENTER THE LONGITUDINAL MATERIAL MODULUS IN PASCALS

?

15D) ENTER THE MATERIAL DENSITY IN KG/CUBIC METERS

?

15E) ENTER THE LONGITUDINAL COEFFICIENT OF THERMAL EXPANSION IN M/M/DEG C

?

15F) ENTER THE CROSS-SECTIONAL AREA OF SURFACE CORD IN SQ. METERS

?

16> TIE-BACK CORD MATERIAL?
(1)-GRAPHITE, (2)-QUARTZ, (3)-OTHER

?

Prompts 16A>, 16D>, and 16E> will appear only if the material desired is other than graphite or quartz.

16A> ENTER THE LONGITUDINAL MATERIAL MODULUS IN PASCALS

?

16D> ENTER THE MATERIAL DENSITY IN KG/CUBIC METERS

?

16E> ENTER THE LONGITUDINAL COEFFICIENT OF THERMAL EXPANSION
IN M/M/DEG C

?

16F> ENTER THE CROSS-SECTIONAL AREA OF SURFACE CORD IN SQ. METERS

?

STANDOFF MATERIAL AND SECTIONAL PROPERTIES

17A> ENTER THE LONGITUDINAL MATERIAL MODULUS IN PASCALS

?

17B> ENTER THE SHEAR MODULUS IN PASCALS

?

17C> ENTER POISSON'S RATIO

?

17D> ENTER THE MATERIAL DENSITY IN KG/CUBIC METERS

?

17E> ENTER THE LONGITUDINAL COEFFICIENT OF THERMAL EXPANSION
IN M/M/DEG C

?

17F> ENTER THE CROSS-SECTIONAL AREA OF SURFACE CORD IN SQ. METERS

?

STANDOFF SECTION INFORMATION
LOCAL Y AXIS IS PARALLEL TO GLOBAL Y AXIS
LOCAL Z AXIS IS PARALLEL TO GLOBAL X AXIS

17G> ENTER THE MOMENT OF INERTIA ABOUT THE LOCAL Y IN METERS**4

?

17H> ENTER THE MOMENT OF INERTIA ABOUT THE LOCAL Z IN METERS**4

?

17I> ENTER THE EXTREME FIBER DISTANCE ABOUT THE LOCAL Y IN METERS
?

17J> ENTER THE EXTREME FIBER DISTANCE ABOUT THE LOCAL Z IN METERS
?

18> WHAT IS THE MAXIMUM CHANGE IN TEMPERATURE IN DEGREES CELSIUS?
?

See section 2.0 of the main report for full usage of this
input parameter.

A.1.1 USER GENERATION SECTION

This section is used when all of the individual box sections are not of identical dimensions.

YOU ARE ALLOWED TO ANALYZE ONLY ONE BOX SECTION OF THE SURFACE.

**X,Y COORDINATES FOR STANDOFF TOP 1
?**

**X,Y COORDINATES FOR STANDOFF TOP 2
?**

**X,Y COORDINATES FOR STANDOFF TOP 3
?**

**X,Y COORDINATES FOR STANDOFF TOP 4
?**

The Z-coordinates for these four standoffs are generated by the program. When these four questions are answered, the program returns to Prompt 5>.

A.2 LOADCASE GENERATOR

NOTE: THIS PROGRAM IS DESIGNED TO BE RUN INTERACTIVELY

Program filenames:

LOADGEN = Source Program
LGENT = Program Listing
LGENB = Binary Program

Local files required before running program:

TAPE16 from the Mesh Tie System Model Generator
TAPE18 from the Mesh Tie System Model Generator

Local files created by the Loadcase Generator:

TAPE3 = Loadcase Deck **

** - indicates files required to be saved for later use

TO RUN PROGRAM

Enter the following system commands after logging onto the system:

GET, LGENB.

MAP, OFF.

GET, TAPE16=pf16, TAPE18=pf18. where "pf1" equals the permanent filename used at the end of the Mesh Tie System Model Generator.

ENDING PROGRAM

Enter the following system commands before logging off the system or continuing to run other programs:

REPLACE, TAPE3=pf3. where "pf1" equals the permanent file name defined above.

PROGRAM PROMPTS

The following statements in **BOLD FACE** print are the computer generated prompts which will appear while running this program:

1) HOW MANY LOADCASES WILL YOU BE GENERATING?

?

For each box section specified for analysis and for the number of loadcases specified in Prompt 1), these prompts will repeat themselves. The following statements will appear whenever either a box section or loadcase is changed:

***** BOX NUMBER xxxx *****
LOADCASE xx

2) LOAD TYPE:

- (0)-DEFINE NEW VALUES FOR CONSTRAINT, FORCE, PRESSURE, AND TEMPERATURE BOUNDARY CONDITIONS
- (1)-USE THE PREVIOUS CONSTRAINTS, FORCES, AND PRESSURE BOUNDARY CONDITIONS AND ADD TEMPERATURE CONDITIONS TO EXISTING MODEL

?

For Loadtype 0, the MAIN MENU appears.
For Loadtype 1, the program bypasses the Main Menu and proceeds directly to the Temperature Creation Section, section A.2.5.

```
*****MENU - LOADTYPE 0*****  
*                                                                    *  
*      1 - Create or Modify Nodal Point Loads                       *  
*      2 - Create or Modify Nodal Constraints                       *  
*      3 - Create or Modify Pressure Loads                         *  
*      4 - Create or Modify Gravity Loads                         *  
*      5 - Create or Modify Temperature Loads                     *  
*      6 - End Loadcase                                           *  
*                                                                    *  
*      Enter numerical choice and <RETURN>                         *  
*                                                                    *  
*****
```

?

The questioning proceeds to the following sections for the following answers:

- 1 - Point Load Creation Section, section A.2.1
- 2 - Constraint Creation Section, section A.2.2
- 3 - Pressure Load Creation Section, section A.2.3
- 4 - G-Load Creation Section, section A.2.4
- 5 - Temperature Creation Section, section A.2.5
- 6 - Ends Loadcase; if there are no more loadcases to be run, proceed to the next box section; if there are no more box sections for which loads must be specified, ends the program.

The screen returns the menu after completing each section.

A.2.1 POINT LOAD CREATION SECTION

The following menu appears for the Point Load Creation Section:

```
*****
*           LOAD MENU           *
*   CRE - CREATE MODAL LOADS   *
*   MOD - MODIFY MODAL LOADS  *
*   LIS - LIST CURRENT STATUS *
*   END - RETURN TO MAIN MENU *
*                               *
*   ENTER MNEMONIC AND <RETURN> *
*****
?
```

A.2.1.1 CREATE NODAL LOADS

For the choice of CRE, the following prompts appear:

- 1) ENTER NODE NUMBER UPON WHICH FORCE(S) IS ACTING
ENTER -1 TO RETURN TO LOAD MENU
?
- 2) ENTER FORCE VALUE
?
- 3) ENTER DIRECTIONS ONE AT A TIME
ENTER <RETURN> TO END
?

These directions are numerical. See section 4.1 in the main report.

- 4) ARE THERE ANY MORE FORCES ON THIS NODE?
?

Answer Y or N. For an answer of Yes, the program returns to Prompt 2).

- 5) ARE THERE OTHER NODES WITH IDENTICAL FORCES AND DIRECTIONS?
?

Answer Y or N. If the answer is Yes, respond to 6). This enables the user to duplicate point loading conditions upon other nodes.

- 6) ENTER NODE NUMBERS
?

7> ARE THERE ANY MORE LOADED NODES?
?

Answer Y or N. If the answer is Yes, the prompts will begin again at Prompt 1>. If the answer is No, return to the Load Menu.

A.2.1.2 MODIFY NODAL LOADS

For the choice of MOD, the following prompts appear:

1) ENTER NODE TO BE MODIFIED
ENTER -1 TO RETURN TO LOAD MENU
?

When the node number is input, the current status of that node will appear.

CURRENT STATUS, NODE 10101

Condition	Force(N or N-m)	Directions
1	120.0000	103000
2	34.6500	000056

This status report is formed from the input given in the creation mode. If the node in question has not been created, and therefore has no status report, the following statement will appear:

CURRENT STATUS, NODE 10101
NODE 10101 NOT CURRENTLY REGISTERED

If the node is registered, the following menu appears:

(1) - ADD CONDITION
(2) - DELETE CONDITION
(3) - CHANGE OR REPLACE CONDITION
(4) - END
ENTER NUMERICAL CHOICE AND <RETURN>
?

1 - Adding a Condition:

This is primarily used when the node is registered and a loading condition is to be added. It is also used when the node is not registered, and allows the user to create loading conditions for the unregistered node from the start.

A1) ENTER FORCE VALUE
?

A2) ENTER DIRECTIONS ONE AT A TIME
ENTER <RETURN> TO END

?

Following the answer to this question, the status report and menu will appear again.

2 - Deleting a Condition:

D1) ENTER CONDITION TO BE DELETED

?

When the condition is deleted, the status report and menu will appear again.

3 - Changing or Replacing a Condition:

Following the answer to this question, the status report and menu will appear again.

C1) ENTER CONDITION TO BE CHANGED

?

C2) ENTER FORCE VALUE

?

C3) ENTER DIRECTIONS ONE AT A TIME
ENTER <RETURN> TO END

?

Following the answer to this question, the status report and menu will appear again.

4 - Ending returns to 1).

A.2.1.3 LIST CURRENT STATUS

For the choice of LIS, the following prompt appears:

1) ENTER NODE TO BE LISTED
ENTER -1 TO RETURN TO LOAD MENU

?

This enables the user to see the status report on a particular node. Following the status report, the program returns to the Load Menu.

A.2.1.4 RETURN TO MAIN MENU

For the choice of END, the program returns to the Main Menu.

A.2.2 CONSTRAINT CREATION SECTION

The following menu appears for the Constraint Creation Section:

```
*****
*           CONSTRAINT MENU           *
*   CRE - CREATE NODAL CONSTRAINTS    *
*   MOD - MODIFY NODAL CONSTRAINTS   *
*   LIS - LIST CURRENT STATUS        *
*   END - RETURN TO MAIN MENU        *
*                                     *
*   ENTER MNEMONIC AND <RETURN>      *
*****
?
```

A.2.2.1 CREATE NODAL CONSTRAINTS

For the choice of CRE, the following prompts appear:

- 1) ENTER NODE NUMBER UPON WHICH CONSTRAINT(S) ACTS
ENTER -1 TO RETURN TO CONSTRAINT MENU
?
- 2) ENTER DISPLACEMENTS IN METERS
?
- 3) ENTER DIRECTIONS ONE AT A TIME
ENTER <RETURN> TO END
?

These directions are numerical. For nodes 6, 7, 8, and 9, i.e., bottoms of the standoffs, directions 4, 5, and 6, i.e., rotations, cannot be applied. See main report.

- 4) ARE THERE ANY MORE CONSTRAINTS ON THIS NODE?
?

Answer Y or N. For a Yes answer, the program returns to Prompt 2). For a No answer, the program returns to Prompt 1).

A.2.2.2 MODIFY NODAL CONSTRAINTS

For the choice of MOD, the following prompts appear:

- 1) ENTER NODE TO BE MODIFIED
ENTER -1 TO RETURN TO CONSTRAINTS MENU
?

When the node number is input, the current status of that node will appear, as shown in the example below.

CURRENT STATUS, NODE 1

Condition	Displacement(m)	Directions
1	0.00005	103000
2	5.1E-07	020000

This status report is formed from the input given in the creation mode. If the node in question has not been created, and therefore has no status report, the following statement will appear:

**CURRENT STATUS, NODE 1
NODE 1 NOT CURRENTLY REGISTERED**

If the node is registered, the following menu appears:

- (1) - ADD CONDITION
- (2) - DELETE CONDITION
- (3) - CHANGE OR REPLACE CONDITION
- (4) - END

**ENTER NUMERICAL CHOICE AND <RETURN>
?**

1 - Adding a Condition:

This is primarily used when the node is registered and a constraining condition is to be added. It is also used when the node is not registered, and allows the user to create constraining loading conditions for the unregistered node from the start.

**A1> ENTER DISPLACEMENT
?**

**A2> ENTER DIRECTIONS ONE AT A TIME
ENTER <RETURN> TO END
?**

Following the answer to this question, the status report and menu will appear again.

2 - Deleting a Condition:

**D1> ENTER CONDITION TO BE DELETED
?**

When the condition is deleted, the status report and menu will appear again.

3 - Changing or Replacing a Condition:

C1) ENTER CONDITION TO BE CHANGED
?

C2) ENTER DISPLACEMENT
?

C3) ENTER DIRECTIONS ONE AT A TIME
ENTER <RETURN> TO END
?

Following the answer to this question, the status report and menu will appear again.

4 - Ending returns to 1).

A.2.2.3 LIST CURRENT STATUS

For the choice of LIS, the following prompt appears:

1) ENTER NODE TO BE LISTED
ENTER -1 TO RETURN TO CONSTRAINT MENU
?

This enables the user to see the status report on a particular node. Following the status report, the program returns to the Constraint Menu.

A.2.2.4 RETURN TO MAIN MENU

For the choice of END, the program returns to the Main Menu.

C-2

A.2.3 PRESSURE LOAD CREATION SECTION

1) INPUT PRESSURES (GLOBAL X,Y,Z) ?

These are input in units of N/m**2
If pressures have already been input, the current pressures
and a new prompt will appear:

CURRENT PRESSURE VECTOR, N/M**2

PRX	PRY	PRZ
xxx	xxx	xxx

1) INPUT NEW PRESSURES (GLOBAL X,Y,Z) ?

A.2.4 G-LOAD CREATION SECTION

1) INPUT ACCELERATION VECTOR (GLOBAL X,Y,Z) ?

These are input in units of m/s**2,

e.g., a 1-G load = 9.81 m/s**2

If accelerations have already been input, the current accelerations and a new prompt will appear:

CURRENT ACCELERATION VECTOR, M/S**2

ACCX	ACCY	ACCZ
xxxx	xxxx	xxxx

1) INPUT NEW ACCELERATION VECTOR (GLOBAL X,Y,Z) ?

NOTE: The forces created by the acceleration vectors act in the opposite direction of the acceleration vector.

A.2.5 TEMPERATURE CREATION SECTION

When entering this section, the current status of the temperatures, such as shown below, appears. If no temperatures have been input for the loadcase, no status report will appear.

CURRENT TEMPERATURE - BOX 101

RECORD	FROM ELEMENT	TO ELEMENT	TEMPERATURE
1	5	78	121.3
2	45	46	100.2
3	79	79	-4.3

THE REFERENCE TEMPERATURE IS 22 DEGREES CELSIUS

Note that record 1 ranges from element 5 through element 78, while record 2 ranges from element 45 through 46, causing an overlap. The result of this is that for elements 5-44 and elements 47-78, the temperature is 121.3 degrees C. For elements 45-46, the temperature is 100.2. Record 3 ranges from element 79 through element 79. This results in element 79 having a temperature of -4.3 degrees C.

If temperatures have been previously defined, the following menu will appear:

- (1) - ADD RECORDS
- (2) - DELETE RECORD
- (3) - CHANGE OR REPLACE RECORD
- (4) - CHANGE REFERENCE TEMPERATURE
- (5) - END

ENTER NUMERICAL CHOICE AND <RETURN>

?

1 - Adding Records:

The prompts in this section are also used to create temperatures for the first time, i.e., when the status and menu do not appear. This section will allow the addition of a number of records.

A1> ENTER TEMPERATURE:

?

A2> FROM ELEMENT # ?

?

A3> TO ELEMENT # ?

?

A4> ARE THERE ANY MORE TEMPERATURE INPUTS?

?

For an answer of Yes, the program returns to Prompt 1).
For an answer of No, the program returns to the status report and menu.

A5> WHAT IS THE REFERENCE TEMPERATURE?

?

Following the answer, the program returns to the status report and menu.

2 - Deleting a Record:

Only one record at a time may be deleted.

D1> ENTER RECORD TO BE DELETED

?

Following the answer, the program returns to the status report and menu.

3 - Changing or Replacing a Record:

C1> ENTER RECORD TO BE CHANGED

?

C2> ENTER TEMPERATURE

?

C3> FROM ELEMENT #

?

C4> TO ELEMENT #

?

Following the answer, the program returns to the status report and menu.

4 - Changing the Reference Temperature:

CREF1> WHAT IS THE REFERENCE TEMPERATURE?

?

Following the answer, the program returns to the status report and menu.

5 - Ending returns to the Main Menu.

A.3 MODEL OPTIMIZER

NOTE: THIS PROGRAM MAY BE RUN IN EITHER INTERACTIVE OR BATCH PROCESS FORM.

Program filenames:

OPMESH = Source Program
OPMESHT = Program Listing
OPMESHB = Binary Program

Local files required before running program:

TAPE16 from the Mesh Tie System Generator
TAPE18 from the Mesh Tie System Generator

Local files created by the Model Optimizer:

TAPE1 = Model Solver Input File **
TAPE2 = First section of Model Solver Output **
TAPE7 = Renumbered node matrix **

** - indicates files required to be saved for later use

TO RUN THE PROGRAM INTERACTIVELY

Enter the following system commands after logging onto the system:

GET, OPMESHB.

MAP, OFF.

GET, TAPE16=pfn16, TAPE18=pfn18. where "pfn" equals the permanent filename used at the end of the Mesh Tie System Model Generator

TO RUN THE PROGRAM BATCH, SEE PAGE A25.

ENDING INTERACTIVE PROGRAM

Enter the following system commands after optimization is complete:

REPLACE, TAPE1=pfn1, TAPE2=pfn2, TAPE7=pfn7. where "pfn" equals the permanent filename defined above.

A.4 FINITE-ELEMENT MODEL SOLVER

NOTE: THIS PROGRAM IS TO BE RUN AS A BATCH PROCESSSS JOB. SEE PAGE A25 FOR THE JOB DECK LISTING USED TO RUN THIS PROGRAM.

Program filenames:

FEMESH = Source Program
FEMESHT = Program Listing
FEMESHB = Binary Program

Local files required before running program:

TAPE1 from the Model Optimizer
TAPE2 from the Model Optimizer
TAPE3 from the Loadcase Generator
TAPE7 from the Model Optimizer

Local files created by the Model Solver:

TAPE2 = Complete Model Solver output **
TAPE20 = Nodal displacements **

** - indicates files required to be saved for later use

A.5 SURFACE TOPOGRAPHY SOLVER

NOTE: THIS PROGRAM IS TO BE RUN AS A BATCH PROCESS JOB. SEE PAGE A25 FOR THE JOB CONTROL LISTING USED TO RUN THIS PROGRAM.

Program filenames:

INTERP = Source Program
INTERPT = Program Listing
INTERPB = Binary Program

Local files required before running program:

TAPE16 from the Tie System Model Generator
TAPE17 from the Tie System Model Generator
TAPE18 from the Tie System Model Generator
TAPE20 from the Finite-Element Model Solver

Local files created by the Surface Topography Solver:

TAPE19 = Displacements of the Surface Node
Points (BINARY)
TAPE29 = Output of information for use in the RF
Performance Program **

** - indicates files required to be saved for later use

A.6 BATCH PROCESSING

To batch process the Model Optimizer, Model Solver, and Surface Topography Solver on the CDC computer, the following JCL deck may be used:

```
job card
user card
charge card
RFL(350000)
REDUCE(-)
MAP,OFF.
GET,OPMESH.
GET,FEMESH.
GET,INTERP.
GET,TAPE3=pf3.
GET,TAPE16=pf16.
GET,TAPE17=pf17.
GET,TAPE18=pf18.
OPMESH.
REWIND,TAPE1,TAPE2,TAPE7.
REPLACE,TAPE1=pf1/NA.
REPLACE,TAPE2=pf2/NA.
REPLACE,TAPE7=pf7/NA.
COPYBF,TAPE2,DUM.
FEMESH.
REWIND,TAPE2,TAPE20.
REPLACE,TAPE2=pf2/NA.
REPLACE,TAPE20=pf20/NA.
REWIND,TAPE16,TAPE18.
INTERP.
REWIND,TAPE29.
REPLACE,TAPE29=pf29/NA.
EXIT.
REWIND,*.
REPLACE,TAPE1=pf1/NA.
REPLACE,TAPE2=pf2/NA.
REPLACE,TAPE7=pf7/NA.
REPLACE,TAPE20=pf20/NA.
REPLACE,TAPE29=pf29/NA.
```

where "pf" equals the user defined permanent filename of five characters which was used after running the Mesh Tie System Model Generator and the Loadcase Generator.

A.7 RF PERFORMANCE SOLVER

NOTE: THIS PROGRAM IS TO BE RUN AS A BATCH PROCESS JOB. TAPE9, WHICH IS REQUIRED TO RUN THE PROGRAM, MUST BE CREATED BY THE USER. TAPE29, WHICH IS THE OUTPUT FROM THE SURFACE TOPOGRAPHY PROGRAM, CONTAINS A CARD IMAGE DECK OF TAPE9 FOR EACH LOADCASE ANALYZED. IF THE USER WISHES TO CREATE THEIR OWN INPUT DECK, THE COMMANDS AND INPUTS FOR EACH COMMAND ARE GIVEN BELOW.

Program filenames:

RFCEF = Source Program
RFCEFT = Program Listing
RFCEFB = Binary Program

Local files required before running program:

TAPE9 to be created by the user

Local files created by the Surface Topography Solver:

TAPE6 = Output of the RF Performance Program **

** - indicates files required to be saved for later use

BATCH PROCESSING

To batch process the RF Performance Solver on the CDC computer, the following JCL deck may be used:

```
job card
user card
charge card
RFL(350000)
REDUCE(-)
MAP,OFF.
GET,RFCEFB.
GET,TAPE9=pf9.
LDSET,PRESET=ZERO.
RFCEFB.
REWIND,TAPE6.
REPLACE,TAPE6=pf6/NA.
EXIT.
REWIND,TAPE6.
REPLACE,TAPE6=pf6/NA.
```

where "pfn" equals the user defined permanent filename of five characters.

The input file of TAPE 9 must be created by the user. A card image deck for each loadcase is in TAPE 29, created by the Surface Topography Solver. The following, taken from the User's Manual created at Ohio State University, describes the method for creating TAPE 9, should the user wish to deviate from the card images:

A. Command DG:

This command enables the user to specify the reflector type and its geometry, i.e., the shape and dimensions of the reflector. The grid size to be used for subdividing the reflector surface and the rectangular grid used for aperture integration is also specified by this command. All units are specified according to the value IUNIT.

1. READ: N TYP

N TYP: This is an integer variable that specifies the reflector type:

PARABOLOIDAL - N TYP=1
SPHERICAL - N TYP=2

2. READ: IUNIT, F, GRIDX, GRIDY, D, N RIM

IUNIT: This is an integer variable that indicates the units for the input data as follows:

METERS - IUNIT=1
FEET - IUNIT=2
INCHES - IUNIT=3

F: This is a real variable which defines the focal length of the parabola.

GRIDX, GRIDY:

These are real variables which define the rectangular grid dimensions, D_x and D_y . The rectangular grid is used for aperture integration and thus its size must be sufficiently small to provide a reasonable piecewise linear representation of the aperture field distribution. However, the grid dimensions may be large in wavelengths. The grid dimensions, D_x and D_y , together with the aperture size control the maximum number of grid lines I_{max} , J_{max} used for aperture integration. At least 20 grid lines must be used in the code. Presently, there can be no less than 20 or more than 200 grid lines in either direction. Note that more grid lines are required when the rotating grid is used for off principal plane cuts. Approximately 50% more grid lines are required for phi-cuts near 45 degrees and odd multiples of 45 degrees.

D: This is a real variable which defines the diameter of the reflector.

NRIM: This is an integer variable which defines the number of input rim points. Presently, NRIM can be no less than 3 and no greater than 127.

B. Command FD:

This command enables the user to specify the feed pattern.

1. READ: NHORN,LFOCUS

NHORN: This is an integer variable which specifies the type of horn feed to be used.

REGULAR HORN FEED - NHORN=1
CORRUGATED HORN FEED - NHORN=2

LFOCUS: This is a logical variable defined by T or F. It is used to tell the code whether the feed is located at the focus or not.

FEED IS FOCUSED - LFOCUS=TRUE
FEED IS DEFOCUSED - LFOCUS=FALSE

2. READ: (DXS(N),N=1,3)

This statement is skipped if LFOCUS=TRUE.

DXS(N):

This is a dimensioned real variable. It is used to specify the displacement of the feed from the focus.

3. READ: ANG1,AW1,ANG2,AW2,AD,TAU

ANG1,ANG2:

These are real variables. They are input in degrees and define the full horn flare angles in the H- and E- planes, respectively.

AW1,AW2:

These are real variables input in the unit specified by the variable IUNIT in the DG: Command. They define the horn aperture widths in the H- and E- planes, respectively.

AD:

This is a real variable in the units specified by IUNIT. It defines the phase reference of the horn as the distance from the horn aperture.

TAU:

This is a real variable. It is input in degrees and defines the linear polarization angle relative to the X-axis of the feed.

VERTICAL POLARIZATION - TAU=90

HORIZONTAL POLARIZATION - TAU=0

C. Command FQ:

This command enables the user to specify the frequencies for which patterns are to be computed.

1. READ: NFRQ,(FREQ(I),I=1,NFRQ)

NFRQ:

This is an integer variable used to define the number of frequency inputs. If the feed is frequency dependent, NFRQ=1, and only one input frequency FREQ(1) is used in conjunction with a new input feed pattern for each frequency, using the FD: Command. Presently, there can be no more than 10 frequencies.

FREQ(I):

This is a dimensioned real variable which defines the Ith frequency in GHz for which a given antenna design with a frequency-

independent feed pattern is to be run.

D. Command TL:

This command enables the user to specify the tilt angle of the feed and the aperture center of the reflector on the X-axis. This information is primarily useful for offset fed reflectors.

1. READ: PHRE, PSTL, PHFD

PHRE: This is the phi-angle between the X-axis of the reflector and the plane of tilt.

PSTL: This is the tilt angle of the antenna.

PHFD: This is the phi-angle between the X-axis of the feed and the plane of tilt.

2. READ: XC, LFDARR

XC: This is a real variable. It is input in the units specified by the variable IUNIT and defines the aperture center of an offset reflector antenna. It is particularly useful for circular rim shapes in which case the rim points are calculated from the reflector diameter, D.

LFDARR:

This is a logical variable defined by T or F. It is used to tell the code whether the line feed array scan option is to be used or not. With this option, the feed location and feed axis tilt are simultaneously adjusted to scan the radiated beam for a spherical reflector.

REGULAR FEED OPTION	LFDARR=FALSE
LINE FEED ARRAY SCAN OPTION	LFDARR=TRUE

E. Command PZ:

This command enables the user to specify the output data. For far field patterns, this command specifies the phi-plane pattern cuts and the initial, final, and incremental values for the pattern angle phi.

1. READ: NTEST2, NTEST3

NTEST2, NTEST3:

These are integer variables which control detailed output data for test purposes. These are normally set to 0.

2. READ: IP2

IP2: This is an integer variable which is used to specify the number of pattern cuts for the output data for each frequency. Its absolute value, NP2=|IP2|, is the number of pattern cuts to be calculated.

3. READ: (AP2(L),L=1, NP2)

This read statement is used for positive values of IP2.

AP2(L):

This is a dimensioned real variable which defines the Lth value of P2 for output pattern data. Presently, there can be no more than 10 cuts.

4. READ: (AP2(L),L=1,2)

This read statement is used for negative values of IP2; then, evenly spaced phi-increments are used as follows:

APL(L):

This is a dimensioned real variable. AP2(1) is the initial value of phi for the output pattern data. AP2(2) is the phi increment for the output pattern data.

5. READ: AP3I, AP3F, ADP3

AP3I: This is a real variable which defines the initial value of the angle off boresight for each pattern cut.

AP3F: This is a real variable which defines the final value of the angle off boresight for each pattern cut.

ADP3: This is a real variable which defines the value by which the angle off boresight is to be incremented for the output pattern.

F. Command XQ:

This command is used to execute the reflector code so that the fields of the reflector may be computed and output. After execution the code returns for another possible command word.

G. Command EF:

This command is used to find the beam efficiency of the antenna. It can be used only for an analysis using four pattern cuts, at phi-angles of 0, 90, 180, and 270.

1. READ: DRUZE,BEF

DRUZE: This is a variable used in the Ruze equation.

$$\text{DRUZE} = 4 \cdot \text{PI} \cdot \text{RMSS} / \text{LAMDA}$$
where RMSS is the rms of system random error.

BEF: This is the beam efficiency of the feed.

H. Command EN:

This ends the program.

Appendix B
Input Data Sheet

APPENDIX B - MESH TIE SYSTEM MODEL GENERATOR INPUT DATA SHEET

Reflector diameter, meters _____

Surface Type, Feed Type _____
 Parabolic-(0), Spherical-(1)
 Center Fed-(0), Offset Fed-(1)

Focal length, meters _____

If Surface Type=1, Spherical radius, meters
 (Enter 0 for default: R=2F) _____

Are all boxes identical (Y or N)? _____

If No, fill out block.

Standoff 1 --- X, Y coordinates, meters _____

Standoff 2 --- X, Y coordinates, meters _____

Standoff 3 --- X, Y coordinates, meters _____

Standoff 4 --- X, Y coordinates, meters _____

Box Type
 Square-(0), Rectangular-(1) _____

If Box Type=0,
 Number of boxes in one side _____

If Box Type=1,
 Number of boxes in X-dir, Y-dir _____

Manufacturing tolerance on the tie system, meters _____

Type of horn feed
 Regular Horn Feed-(1), Corrugated Horn Feed-(2) _____

Edge taper of the feed, dB _____

Frequency of operation, GHz _____

Do you want a plot of the box truss system (Y or N) _____

Standoff height -- Program will automatically calculate
 optimum standoff height. If you have particular
 design requirements, input new standoff height, meters. _____

Interpolation technique
 Worst Case-(0), 1-D Linear-(1), 2-D Linear-(2) -----

If Technique=0,
 Box Number to be analyzed -----

If Technique=1 or 2,
 Box Numbers to be interpolated between -----

Number of shadowed boxes - Not applicable to
 worst-case analysis technique -----

Shadow box numbers - Not applicable to
 worst-case analysis technique or
 zero shadow boxes. -----

If Technique=1,
 Direction of interpolation (X or Y) -----

Nominal tie spacing, meters -----

Do you want tie desing printed to screen (Y or N) -----

Do you want a plot of the tie system (Y or N) -----

Percent of model to be analyzed, % -- Best answered
 when running the program. -----

SURFACE CORD MATERIAL
 Graphite-(1), Quartz-(2), Other-(3) -----

If Material=3,
 Mcdulus, Pa -----

CTE, m/m/deg C -----

Density, kg/cubic meter -----

Cross-sectional area of surface cord, square meters -----

TIEBACK CORD MATERIAL
 Graphite-(1), Quartz-(2), Other-(3) -----

If Material=3,
 Modulus, Pa -----

CTE, m/m/deg C -----

Density, kg/cubic meter -----

Cross-sectional area of tie-back cord, square meters -----

STANDOFF INFORMATION
 Material modulus, Pa -----

Material shear modulus, Pa	-----
Poisson's ratio	-----
Material density, kg/cubic meter	-----
Material CTE, m/m/deg C	-----
Cross-sectional area, square meters	-----
Moment of inertia-Local Y, meters 4	-----
Moment of inertia-Local Z, meters 4	-----
Extreme fiber thickness-Local Y, meters	-----
Extreme fiber thickness-Local Z, meters	-----
Maximum temperature change, degrees C (See Section 2.0 for full usage of this input parameter.)	-----

1. Report No. NASA CR-172570	2. Government Accession No.	3. Recipient's Catalog No.	
4. Title and Subtitle Box Truss Analysis and Technology Development Task 1 -- Mesh Analysis and Control		5. Report Date August 1985	
		6. Performing Organization Code	
7. Author(s) E. E. Bachtell, S. S. Bettadapur, J.V. Coyner		8. Performing Organization Report No. MCR - 85 - 533	
		10. Work Unit No.	
9. Performing Organization Name and Address Martin Marietta Denver Aerospace P.O. Box 179 Denver, Colorado 80201		11. Contract or Grant No. NAS1-17551	
		13. Type of Report and Period Covered Contractor Report	
12. Sponsoring Agency Name and Address National Aeronautics and Space Administration Washington, D.C. 20546		14. Sponsoring Agency Code	
		15. Supplementary Notes Langley Technical Monitor: Uriel M. Lovelace Final Report - Task 1	
16. Abstract An analytical tool was developed to model, analyze and predict rf performance of box truss antennas with reflective mesh surfaces. The analysis system is unique in that it integrates custom written programs for cord tied mesh surfaces, thereby drastically reducing the cost of analysis. The analysis system is capable of determining the rf performance of antennas under any type of manufacturing or operating environment by integrating together the various disciplines of design, finite-element analysis, surface "best-fit" analysis and rf analysis. The Integrated Mesh Analysis System consists of six separate programs: The Mesh Tie System Model Generator, The Loadcase Generator, The Model Optimizer, The Model Solver, The Surface Topography Solver and The RF Performance Solver. Additionally, a study using the mesh analysis system was performed to determine the effect of on-orbit calibration, i.e., surface adjustment, on a typical box truss antenna.			
17. Key Words (Suggested by Author(s)) Large Space Structures Antennas Mesh Reflectors		18. Distribution Statement Unclassified - Unlimited	
19. Security Classif. (of this report) Unclassified	20. Security Classif. (of this page) Unclassified	21. No. of Pages 115	22. Price